

## REFERENCES

- Ahmad, H., Kamarudin, S.K., Hasran, U.A., and Daud, W.R.W. (2010). Overview of hybrid membranes for direct-methanol fuel-cell applications. International Journal of Hydrogen Energy, 35, 2160–2175.
- Ahmad, M.I., Zaidi, S.M.J., and Rahman, S.U. (2006). Proton conductivity and characterization of novel composite membranes for medium-temperature fuel cells. Desalination, 193, 387–397.
- Aliabadi, M., Ebadi, M., Dashtimoghadam E., Mirsasaani, S., Majedi F.S., and Sadrabadi, M.M.H. (2011). Nanocomposite Proton Exchange Membranes Based on Sulfonated Poly (2,6-Dimethyl-1,4-Phenylene Oxide) with Enhanced Performance for Fuel Cell Applications. Journal of Macromolecular Science, 50, 1108–1120.
- Baglio, V., Arico, A.S., Blasi, A.D., Antonucci, P.L., Nannetti, F., Tricoli, V., and Antonucci, V. (2005). Zeolite-based composite membranes for high temperature direct methanol fuel cells. Journal of Applied Electrochemistry, 35, 207–212.
- Bozbag, S.E., and Erkey, C. (2012). Supercritical fluids in fuel cell research and development. Journal of Supercritical Fluids, 62, 1-31.
- Deligoz H, Vantansever S, Koc S.N., Oksuzomer F, Ozgumus S, and Gurkaynak M.A. (2008). Preparation of Sulfonated Copolyimides Containing Aliphatic Linkages as Proton-Exchange Membranes for Fuel Cell Applications. Journal of Applied Polymer Science, 110, 1216-1224.
- Fu, R.Q., Julius, D., Hong, L., and Lee, J.Y. (2008). PPO-based acid–base polymer blend membranes for direct methanol fuel cells. Journal of Membrane Science, 322, 331–338.
- Fu, Y.Z., and Manthiram, A. (2006). Synthesis and characterization of sulfonated polysulfone membranes for direct methanol fuel cells. Journal of Power Sources, 157, 222–225.

- Haghighi, A.H., Sadrabadi, M.M.H., Dashtimoghadam, E., Bahlakeh, G., Shakeri, S.E., Majedi, F.S., Emami, S.H., and Moaddel, H. (2011). Direct methanol fuel cell performance of sulfonated poly (2,6-dimethyl-1,4-phenylene oxide)-polybenzimidazole blend proton exchange membranes. INTERNATIONAL JOURNAL OF HYDROGEN ENERGY, 36, 3688-3696.
- Holmberg, B.A., Wang, X., and Yan, Y. (2008). Nanocomposite fuel cell membranes based on Nafion and acid functionalized zeolite beta nanocrystals. Journal of Membrane Science, 320, 86–92.
- Intaraprasit, N., Kongkachuichay, P. (2011). Preparation and properties of sulfonated poly(ether ether ketone)/Analcime composite membrane for a proton exchange membrane fuel cell (PEMFC). Journal of the Taiwan Institute of Chemical Engineers, 42, 190–195.
- Jung, B., Ki, B., and Yang, J.M. (2004). Transport of methanol and protons through partially sulfonated polymer blend membranes for direct methanol fuel cell. Journal of Membrane Science, 245, 61–69.
- Kang, S., Zhang, C., Xiao, G., Yan, D., and Sun, G. (2009). Synthesis and properties of soluble sulfonated polybenzimidazoles from 3,3'-disulfonate-4,4'-dicarboxylbiphenyl as proton exchange membranes. Journal of Membrane Science, 334, 91-100.
- Ko, H., Yu, D.M., Choi, J., Kim, H., and Hong, Y. (2012). Synthesis and characterization of intermolecular ionic cross-linked sulfonated poly(arylene ether sulfone)s for direct methanol fuel cells. Journal of Membrane Science, 390–391, 226–234.
- Kobayashi, T., Rikukawa, M., Sanui, K., and Ogata, N. (1988). Proton-conducting polymers derived from poly(ether-etherketone) and poly(4-phenoxybenzoyl-1,4-phenylene). Solid State Ionics, 106, 219–225.
- Li, C., Liu, J., Guan, R., Zhang, P., and Zhang, Q. (2007). Effect of heating and stretching membrane on ionic conductivity of sulfonated poly(phenylene oxide). Journal of Membrane Science, 287, 180–186.

- Lufrano, F., Baglio, V., Staiti, P., Arico, A.S., and Antonucci, V. (2006). Development and characterization of sulfonated polysulfone membranes for direct methanol fuel cells. Desalination, 199, 283–285.
- Lufrano, F., Baglio, V., Staiti, P., Arico, A.S., and Antonucci, V. (2008). Polymer electrolytes based on sulfonated polysulfone for direct methanol fuel cells. Journal of Power Sources, 179, 34–41.
- Macksasitorn, S., Changkhamchom, S., Sirivat, A., and Siemanond, K. (2012). Sulfonated poly(ether ether ketone) and sulfonated poly(1,4-phenylene ether ether sulfone) membranes for vanadium redox flow batteries. High Performance Polymers, 24(7), 603-608.
- Park, H.B., Lee, C.H., Sohn, J.Y., Lee, Y.M., Freeman, B.D., and Kim, H.J. (2006). Effect of crosslinked chain length in sulfonated polyimide membranes on water sorption, proton conduction, and methanol permeation properties. Journal of Membrane Science, 285, 432-443.
- Peighambardoust, S.J., Rowshanzamir, S., and Amjadi, M. (2010). Review of the proton exchange membranes for fuel cell applications. International Journal of Hydrogen Energy, 35, 9349-9384.
- Petreanu, I., Ebrasu, D., Sisu, D., and Varlam, M. (2012). Thermal analysis of sulfonated polymers tested as polymer electrolyte membrane for PEM fuel cells. Journal of Thermal Analysis and Calorimetry, 110, 335–339.
- Rusanov, A.L., Likhatchev, D., Kostoglodov, P.V., Mullen, K., and Klapper, M. (2005). Proton-Exchanging Electrolyte Membranes Based on Aromatic Condensation Polymers. Advances in Polymer Science, 179, 83–134.
- Sadrabadi, M.M.H., Emami, S.H., Moaddel, H. (2008). Preparation and characterization of nanocomposite membranes made of poly(2,6-dimethyl-1,4-phenylene oxide) and montmorillonite for direct methanol fuel cells. Journal of Power Sources, 183, 551–556.
- Sadrabadi, M.M.H., Ghaffarian, S.R., Dorri, N.M., Dashtimoghadam, E., and Majedi, F.S. (2009). Characterization of nanohybrid membranes for direct methanol fuel cell applications. Solid State Ionics, 180, 1497–1504.

- Seol, J.H., Won, J.H., Yoon, K.S., Hong, Y.T., and Lee, S.Y. (2012). SiO<sub>2</sub> ceramic nanoporous substrate-reinforced sulfonated poly(arylene ether sulfone) composite membranes for proton exchange membrane fuel cells. International Journal of Hydrogen Energy, 37, 76189-6198.
- Uctug, F.G., and Holmes, S.M. (2011). Characterization and fuel cell performance analysis of polyvinylalcohol–mordenite mixed-matrix membranes for direct methanol fuel cell use. Electrochimica Acta, 56, 8446– 8456.
- Unveren, E.E., Erdogan, T., Celebi, S.S., and Inan T.Y. (2010). Role of post-sulfonation of poly(ether ether sulfone) in proton conductivity and chemical stability of its proton exchange membranes for fuel cell. International Journal of Hydrogen Energy, 35, 3736 – 3744.
- Vielstich, W., Lamm, A., Gasteiger, H.A. (2003). Automotive development. In Handbook of Fuel Cells-Fundamentals, Technology and Applications. New York: Wiley. (pp. 1217-1223).
- Wang, Y., Jiang, Z., Li, H., and Yang, D. (2010). Chitosan membranes filled by GPTMS-modified zeolite beta particles with low methanol permeability for DMFC. Chemical Engineering and Processing, 49, 278–285.
- Wang, Y., Yang, D., Zheng, X., Jiang, Z., and Li, J. (2008). Zeolite beta-filled chitosan membrane with low methanol permeability for direct methanol fuel cell. Journal of Power Sources, 183, 454–463.
- Wen, S., Gong, C., Tsen, W.C, Shu, Y.C., and Tsai, F.C. (2009). Sulfonated poly(ether sulfone) (SPES)/boron phosphate (BPO<sub>4</sub>) composite membranes for high-temperature proton-exchange membrane fuel cells. INTERNATIONAL JOURNAL OF HYDROGEN ENERGY, 34, 8982 – 8991.
- Woo, Y., Oh, S.Y., Kang, Y.S., and Jung, B. (2003). Synthesis and characterization of sulfonated polyimide membranes for direct methanol fuel. Journal of Membrane Science, 220, 31-35.
- Wu, H., Zheng, B., Zheng, X., Wang, J., Yuan, W., and Jiang, Z. (2007). Surface-modified Y zeolite-filled chitosan membrane for direct methanol fuel cell. Journal of Power Sources, 173, 842–852.

- Xu, T., Wu, D., and Wu, L. (2008). Poly(2,6-dimethyl-1,4-phenylene oxide) (PPO)—A versatile starting polymer for proton conductive membranes (PCMs). Progress in Polymer Science, 33, 894–915.
- Yang, H.N., Lee J.Y., Jeong, J.Y., Na, Y., and Kim W.J. (2011). Cell performance of DMFC fabricated with H<sup>+</sup>-ETS-10/Nafion composite membrane. Microporous and Mesoporous Materials, 143, 215–220.
- Yang, S., Gong, C., Guan, R., Zou, H., and Dai, H. (2006). Sulfonated poly(phenylene oxide) membranes as promising materials for new proton exchange membranes. POLYMERS FOR ADVANCED TECHNOLOGIES, 17, 360–365.
- Yildirim, M. H., Curos, A.R., Motuzas, J., Julbe, A., Stamatialis, D.F., and Wessling, M. (2009). Nafion<sup>®</sup>/H-ZSM-5 composite membranes with superior performance for direct methanol fuel cells. Journal of Membrane Science, 338, 75–83.
- Zaidi, S.M.J., Bello, M., and Rahman, S.U. (2007). Evaluation of Methanol Crossover through SPEEK/TPA/Y-zeolite Composite Membranes by Electrochemical Method. ECS Transactions, 5 (1), 69-78.
- Zhai F, Gou X, Fang J, and Xu H. (2007). Synthesis and properties of novel sulfonated polyimide membranes for direct methanol fuel cell application. Journal of Membrane Science, 296, 102-109.
- Zhang, Z., Desilets, F., Felice, V., Mecheri, B., Licocchia, S., and Tavares, A.C. (2011). On the proton conductivity of Nafion–Faujasite composite membranes for low temperature direct methanol fuel cells. Journal of Power Sources, 196, 9176–9187.

## APPENDICES

### Appendix A Fourier Transform Infrared Spectrometer (FTIR)

FTIR spectrometer (Thermo Nicolet, Nexus 670) was used to study the chemical structures of poly(2,6-dimethyl-1,4-phenylene oxide) (PPO) and sulfonated poly(2,6-dimethyl-1,4-phenylene oxide) (SPPO). The spectrometer was operated in the transmittance mode in the wave number range  $400\text{-}4000\text{cm}^{-1}$ . Optical grade KBr was used as the background material. PPO and SPPO are mixed with KBr before the measurement.

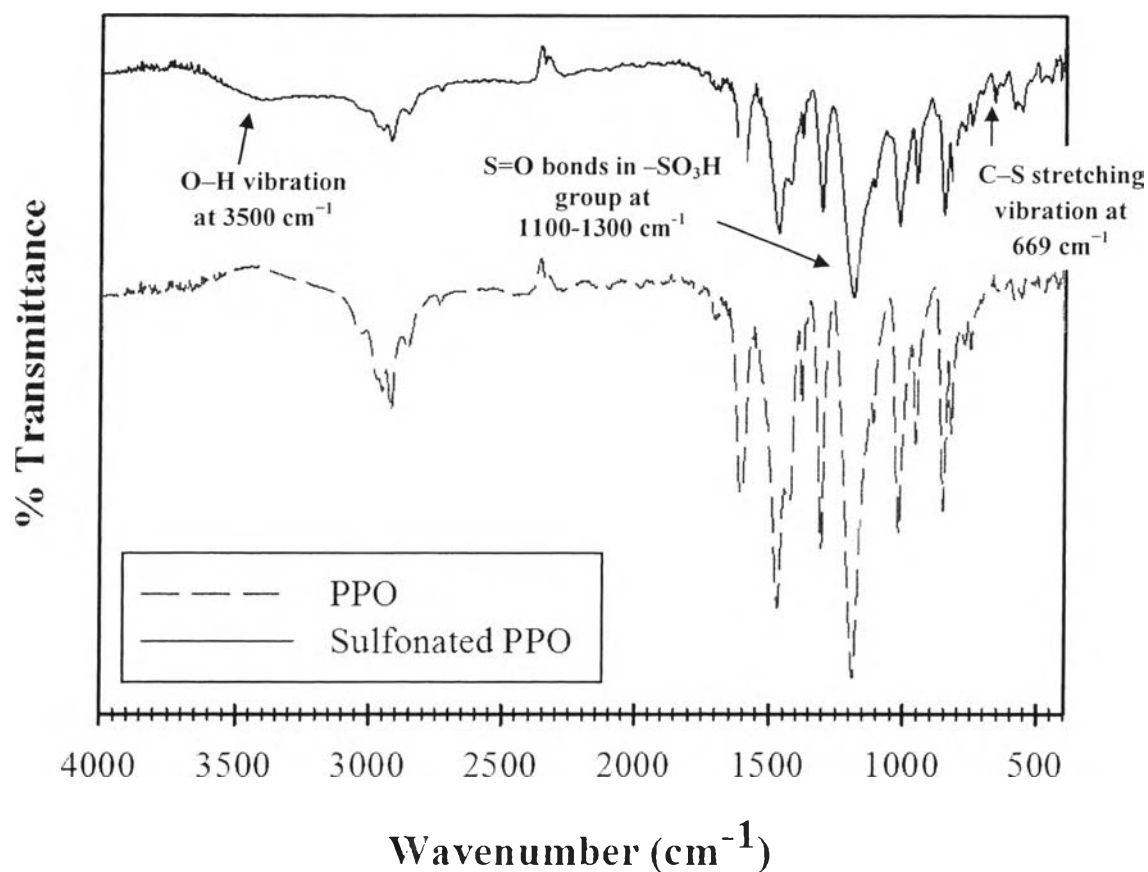


Figure A1 FTIR spectrum of PPO and SPPO.

The FTIR spectra of PPO and SPPO and are shown in comparison in Figure A1, indicating characteristic bands of the pendant sulfonic groups ( $-\text{SO}_3\text{H}$ ) on the polymer chains. Some peaks such as 3500 and 669  $\text{cm}^{-1}$  appear after sulfonation, the characteristic transmittance peaks at 1060 and 1100-1300  $\text{cm}^{-1}$  (broad peak) in SPPO indicate the S=O bonds, and the peak at 1060  $\text{cm}^{-1}$  corresponds to the symmetric stretching band of the aromatic  $-\text{SO}_3\text{H}$  group, and the peak at 669  $\text{cm}^{-1}$  is due to the C-S stretching vibration. The broad band in the SPPO samples at around 3500  $\text{cm}^{-1}$  can be assigned to the O-H vibration. From the result, sulfonic groups have been introduced successfully into the polymer backbone (Li *et al.*, 2007, Sadrabadi *et al.*, 2008).

**Table A1** Characterization of FTIR spectrum of SPPO

Wavenumber ( $\text{cm}^{-1}$ )	Assignment	References
669	C-S stretching vibration	Sadrabadi <i>et al.</i> , 2008, Li <i>et al.</i> , 2007
1100-1300	S=O bonds in $-\text{SO}_3\text{H}$ group	Sadrabadi <i>et al.</i> , 2008, Li <i>et al.</i> , 2007
3500	O-H vibration	Sadrabadi <i>et al.</i> , 2008, Li <i>et al.</i> , 2007

## Appendix B Thermogravimetric Analysis (TGA)

Thermogravimetric analysis (TGA, G50) was used to determine the thermal stability of PPO and SPPO. The membranes were dried in vacuum for 24 hours to remove any moisture in the membranes. The experiment was carried out by weighting a membrane sample of 4-20 mg and placed it in an platinum pan. The sample pan was heated under nitrogen atmosphere from 30 to 800 °C with a heating rate 10 °C/min.

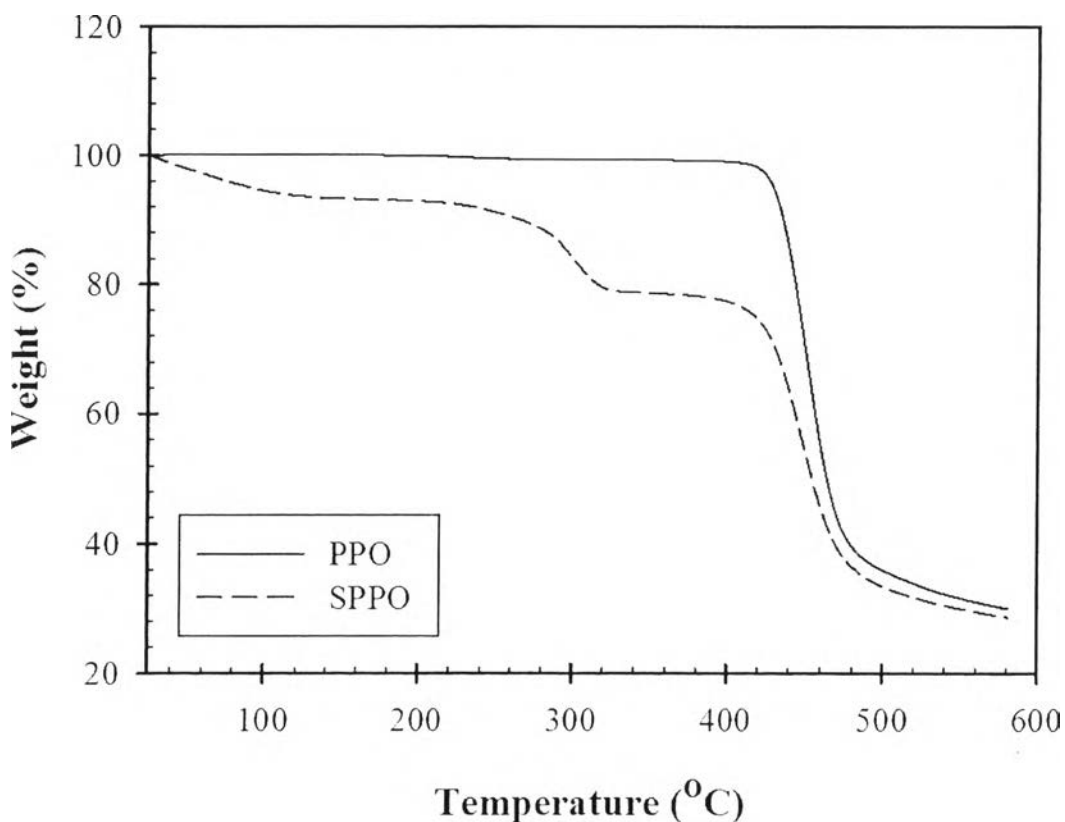


**Figure B1** TGA curve of PPO and SPPO.

Figure B1 shows the thermal stabilities of PPO and SPPO. PPO begins to lose weight at 480 °C, which is owing to the degradation of the polymer chain. Three main weight loss stages can be exhibited for SPPO. The first weight loss is located at 50-100 °C, which is related to the desorption of moisture bonded to the hydrophilic



sulfonic groups ( $-\text{SO}_3\text{H}$ ). The second stage weight loss starts at 200-260 °C, which could be caused by the decomposition of the sulfonic groups. And the final weight loss is close at 420-480 °C, which may be due to the polymer main chain degradation (Li *et al.*, 2007).

**Table B1** Characterization of TGA curve of SPPO

Temperature (°C)	Assignment	references
50-100	Desorption of moisture bonded to the sulfonic groups ( $-\text{SO}_3\text{H}$ )	Li <i>et al.</i> , 2007, Smitha <i>et al.</i> , 2003
200-260	Decomposition of sulfonic groups ( $-\text{SO}_3\text{H}$ )	Li <i>et al.</i> , 2007, Smitha <i>et al.</i> , 2003
420-480	The degradation of the polymer main chain	Li <i>et al.</i> , 2007, Smitha <i>et al.</i> , 2003

### Appendix C Degree of Sulfonation (DS)

Degree of sulfonation is defined as the number of sulfonic groups per repeating units in polymer chain. The polymer membranes were acidified by 2 M HCl solution at room temperature for 24 hours. Then the membranes were dried at 60 °C for 24 hours. After that the membranes were placed in a NaCl solution for 24 hours. And then, the solution was titrated with 0.01 M NaOH by using phenolphthalein as an indicator. Degree of Sulfonation was calculated by the following equation:

$$DS = \frac{(V_{\text{NaOH}} \times M_{\text{NaOH}})/1000}{\text{Mole of polymer membrane}} \times 100 \quad (\text{C1})$$

where DS is the degree of sulfonation (%),  $V_{\text{NaOH}}$  is the volume of NaOH consumed (ml), and  $M_{\text{NaOH}}$  is the molarity of NaOH.

**Table C1** Degree of sulfonation of SPPO membranes with various amount of concentrated sulfuric acid

Amount of conc. H <sub>2</sub> SO <sub>4</sub> (ml)	Degree of Sulfonation (%)			Average (%)	STD.
23.33	19.23	18.13	19.23	18.86	0.64
46.67	23.27	24.26	24.26	23.93	0.57
116.67	30.34	29.49	30.34	30.06	0.49
233.33	30.45	32.27	32.27	31.66	1.05
583.33	30.10	33.16	31.12	31.46	1.56

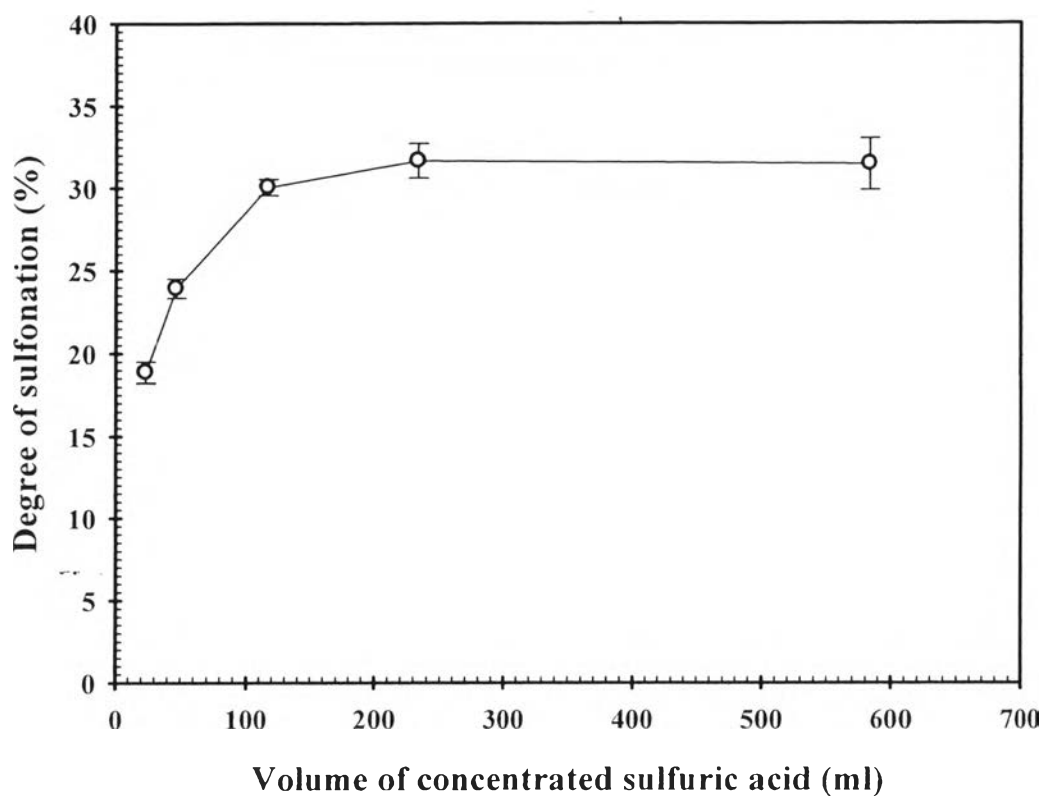


**Figure C1** Degree of sulfonation of SPPO as a function of amount of concentrated sulfuric acid.

Poly(1,4-phenylene sulfide) (PPS) was dissolved in many solvent at various temperature as shown in Table C3. As a result, PPS cannot be dissolved in any solvent.

**Table C2** The solubility of polyphenylene sulfide (PPS)

PPS	Solvents (20 ml)	Boiling point of solvent (°C)	Temperature for dissolving (°C)	Remark
0.20 g	Dimethylformamide	153.0	120	Insoluble
0.20 g	Dimethylacetide	166.1	120	Insoluble
0.20 g	Dimethylsulfoxide	189.0	120	Insoluble
0.20 g	Toluene	110.6	120	Insoluble
0.20 g	Conc. sulfuric acid	337.0	120	Insoluble
0.20 g	N-Methyl-2-pyrrolidone	202.0	120	Insoluble
0.20 g	Tetrahydrofuran	66.0	30	Insoluble
0.20 g	Chloroform	61.2	30	Insoluble
0.20 g	Dichloroethane	39.8	30	Insoluble

## Appendix D Ion Exchange Capacity

Ion exchange capacity (IEC) of the SPPO membranes was measured by a titration. The membranes were cut into small pieces. Then the membranes were immersed into 1 M NaCl solution for 24 hours. The solution was titrated with 0.01 M NaOH solution. Phenolphthalein was used as an indicator. Ion exchange capacity was calculated from following equation:

$$\text{IEC} = \frac{\text{Consumed NaOH} \times \text{molarity NaOH}}{W_{\text{dry}}} \quad (\text{D1})$$

where IEC is the ion exchange capacity (meq/g),  $V_{\text{NaOH}}$  refers to the volume of sodium hydroxide solution,  $C_{\text{NaOH}}$  refers to the concentration of sodium hydroxide solution.

**Table D1** Ion exchange capacity of SPPO membranes with various sulfonation degree

Polymer	IEC (meq/g)			Average (meq/g)	STD.
SPPO, DS = 18.86	1.11	1.21	1.21	1.18	0.06
SPPO, DS = 23.93	1.22	1.39	1.39	1.33	0.10
SPPO, DS = 30.06	1.71	1.66	1.66	1.68	0.03
SPPO, DS = 31.66	1.69	1.76	1.76	1.74	0.04
SPPO, DS = 31.46	1.76	1.70	1.76	1.74	0.03
Nafion 117 (Woo <i>et al.</i> , 2003)	-	-	-	0.91	-

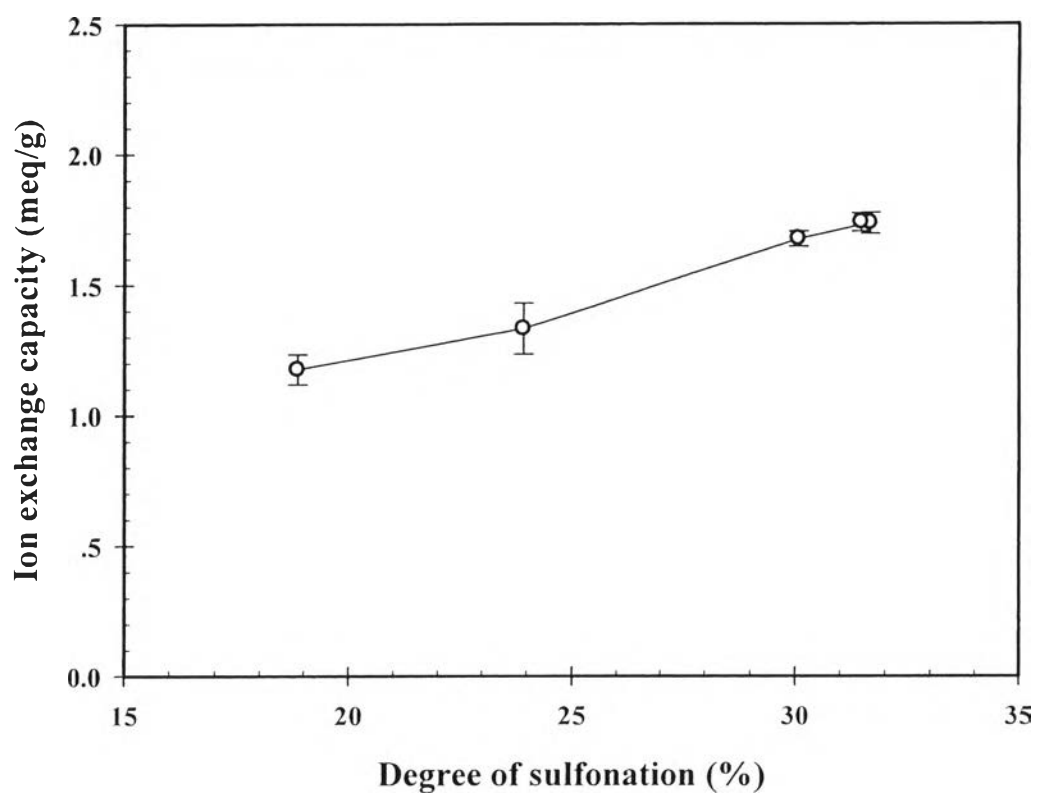


**Figure D1** Ion exchange capacity of SPPO as a function of degree of sulfonation.

## Appendix E Water Uptake

The SPPO membranes were dried in an oven at 100 °C for 24 hours, weighed, and placed into distilled water overnight at room temperature. After that, the membranes were taken out, quickly wiped with a tissue paper. The membranes were weighed again. The water uptake of SPO membrane was calculated from the following equation:

$$\text{Water uptake} = \frac{W_{\text{wet}} - W_{\text{dry}}}{W_{\text{dry}}} \times 100\% \quad (\text{E1})$$

where  $W_{\text{wet}}$  and  $W_{\text{dry}}$  refer to the weights of the wet and dry samples, respectively.

**Table E1** Water uptake of SPPO membranes with various sulfonation degree

Polymer	Water uptake (%)			Average (%)	STD.
SPPO, 18.86	10.34	10.71	9.89	10.32	0.41
SPPO, 23.93	12.64	12.94	13.33	12.97	0.35
SPPO, 30.06	14.81	13.51	12.73	13.69	1.05
SPPO, 31.66	13.74	14.29	15.84	14.62	1.09
SPPO, 31.46	15.48	14.13	13.04	14.22	1.22
Nafion 117 (Woo <i>et al.</i> , 2003)	-	-	-	34.21	-

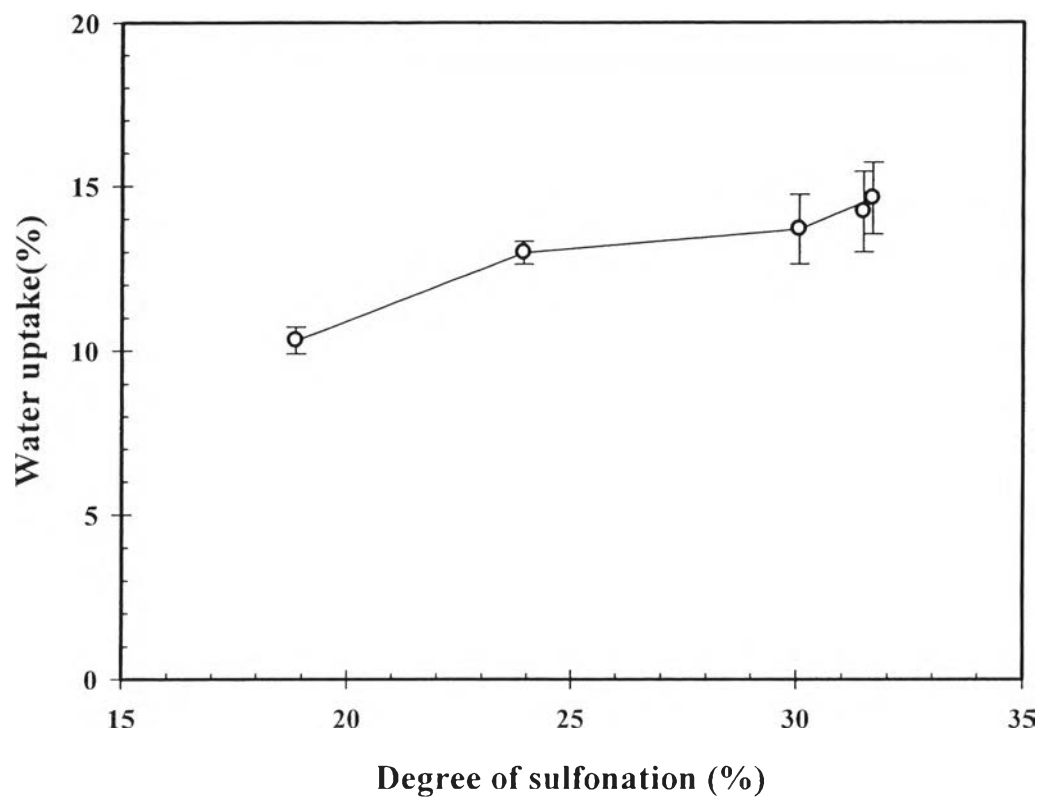


**Figure E1** Water uptake of SPPO as a function of degree of sulfonation.

**Table E2** Water uptake of composite membranes at various concentrations

Composite membranes (%v/v)	Water uptake (%)			Average (%)	STD.
SPPO, DS = 31	13.74	14.29	15.84	14.62	1.09
CM 0.1 %	13.10	13.75	12.20	13.01	0.78
CM 0.5 %	12.33	11.69	11.39	11.80	0.48
CM 1%	9.09	9.62	9.47	9.39	0.27
CM 2%	8.89	9.52	8.99	9.13	0.34



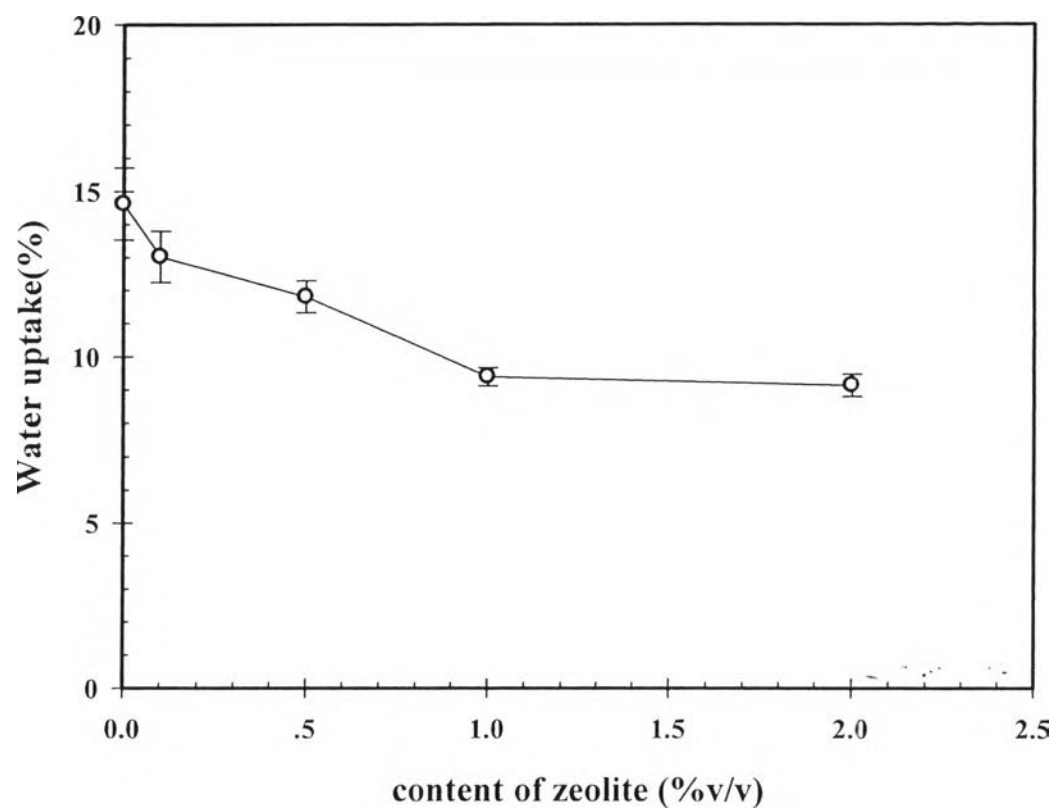


**Figure E1** Water uptake of composite membrane as a function of content of zeolite.

## Appendix F Proton Conductivity

The proton conductivity of the membranes was measured by using Agilent E4980A LCR meter. The fully hydrated membrane was cut into  $0.5 \times 0.5$  cm pieces and coated with silver. The coated membrane was measured at a 1V, and using the alternating current in the frequency range of 20 Hz – 2 MHz. The conductivity was calculated from the impedance as follow:

$$\sigma = \frac{d}{R \times A} \quad (F1)$$

where  $\sigma$  is the proton conductivity (S/cm),  $d$  is the thickness of the membrane,  $S$  is the area of the interface of membrane in contact with the electrodes, and  $R$  refers to the measured resistance of the membrane – derived from the low frequency semicircle on the complex impedance plane with the  $Z$  axis (Park *et al.*, 2006).

**Table F1** Proton conductivity of SPPO and composite membranes at various concentrations

Composite membranes (%v/v)	Proton Conductivity (S/cm)			STD.
	No.1	No.2	Average	
SPPO, DS = 31	$1.04 \times 10^{-2}$	$9.67 \times 10^{-3}$	$1.00 \times 10^{-2}$	$1.63 \times 10^{-4}$
CM 0.1 %	$7.23 \times 10^{-3}$	$7.45 \times 10^{-3}$	$7.34 \times 10^{-3}$	$5.26 \times 10^{-4}$
CM 0.5 %	$5.76 \times 10^{-3}$	$5.85 \times 10^{-3}$	$5.80 \times 10^{-3}$	$1.56 \times 10^{-4}$
CM 1 %	$5.60 \times 10^{-3}$	$5.58 \times 10^{-3}$	$5.59 \times 10^{-3}$	$6.58 \times 10^{-5}$
CM 2 %	$4.43 \times 10^{-3}$	$4.66 \times 10^{-3}$	$4.54 \times 10^{-3}$	$1.12 \times 10^{-5}$
Nafion 117 (Woo <i>et al.</i> , 2003)	-	-	$1.00 \times 10^{-1}$	-

CM = Composite membrane

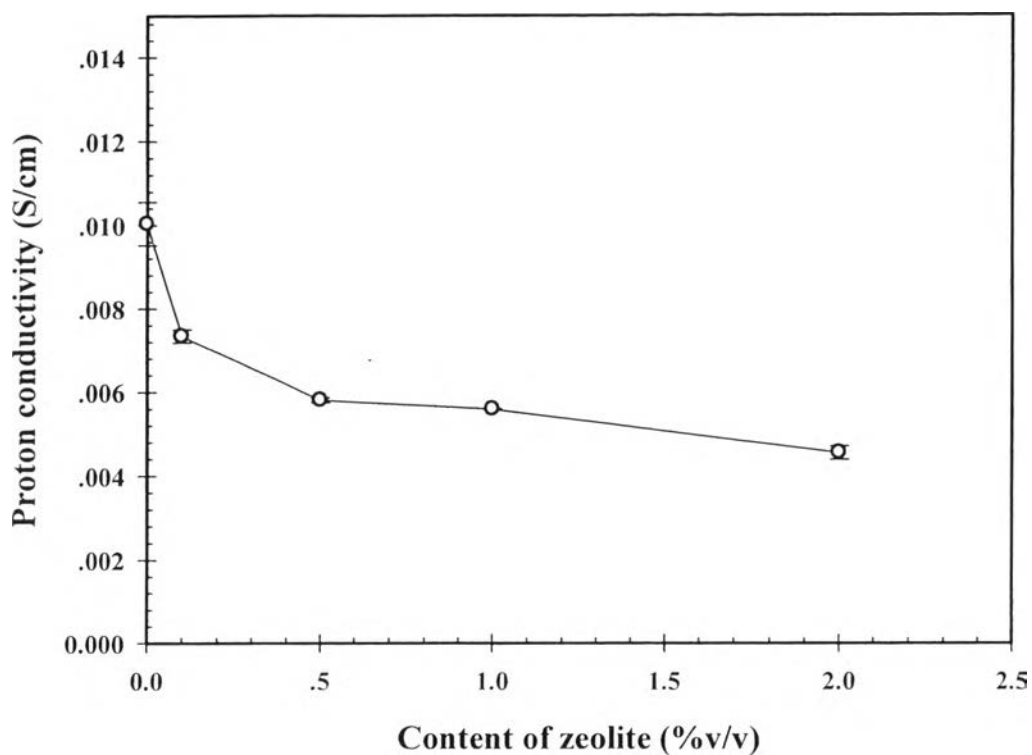


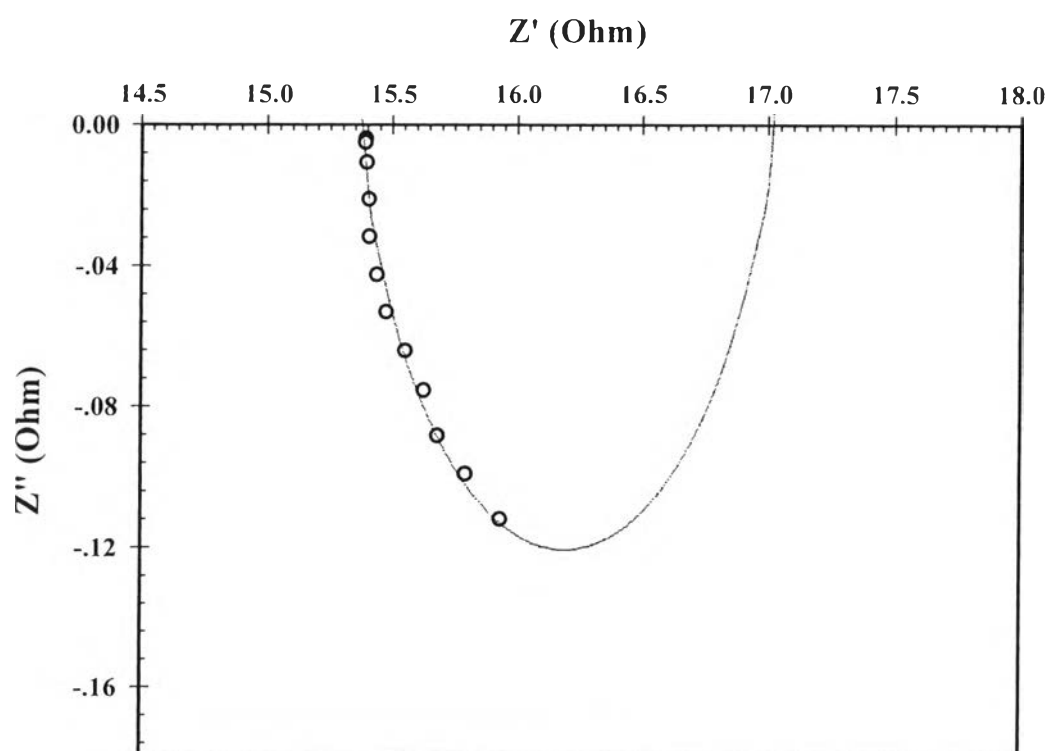
**Figure F1** The proton conductivity of composite membranes as a function of content of zeolite.

**Table F2** Raw data of Proton conductivity calculations

Polymer	Thickness (cm)	Area (cm <sup>2</sup> )	R (ohm)	Proton conductivity (S/cm)
CM 0.1 %	$1.72 \times 10^{-2}$	$9.62 \times 10^{-2}$	14.28	$7.23 \times 10^{-3}$
	$1.72 \times 10^{-2}$	$9.62 \times 10^{-2}$	15.38	$7.45 \times 10^{-3}$
CM 0.5 %	$1.60 \times 10^{-2}$	$9.62 \times 10^{-2}$	24.73	$5.76 \times 10^{-3}$
	$1.60 \times 10^{-2}$	$9.62 \times 10^{-2}$	24.00	$5.85 \times 10^{-3}$
CM 1 %	$1.90 \times 10^{-2}$	$9.62 \times 10^{-2}$	28.90	$5.60 \times 10^{-3}$
	$1.90 \times 10^{-2}$	$9.62 \times 10^{-2}$	28.44	$5.58 \times 10^{-3}$
CM 2 %	$2.31 \times 10^{-2}$	$9.62 \times 10^{-2}$	35.30	$4.43 \times 10^{-3}$
	$2.31 \times 10^{-2}$	$9.62 \times 10^{-2}$	35.40	$4.66 \times 10^{-2}$
SPPO, DS = 31	$1.43 \times 10^{-2}$	$9.62 \times 10^{-2}$	14.28	$1.04 \times 10^{-2}$
	$1.43 \times 10^{-2}$	$9.62 \times 10^{-2}$	15.38	$9.67 \times 10^{-3}$

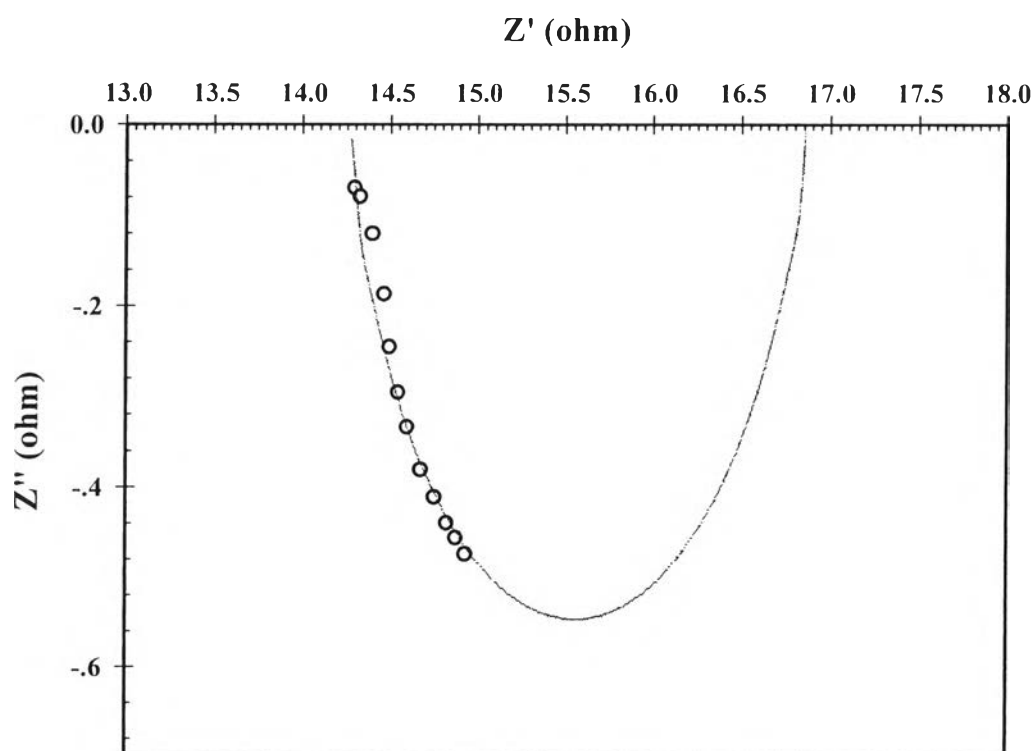
**Table F3** Proton conductivity raw data of calculations SPPO, DS = 31 membrane

Frequency, Hz	Z, ohm	r, Radian	Z'=Zcosr	Z''=Zsinr
80000	15.39	-2.75E-04	15.39	-0.004
100000	15.39	-3.44E-04	15.39	-0.005
200000	15.40	-7.10E-04	15.40	-0.011
400000	15.41	-1.39E-03	15.41	-0.021
600000	15.41	-2.07E-03	15.41	-0.032
800000	15.44	-2.77E-03	15.44	-0.043
1000000	15.48	-3.45E-03	15.48	-0.053
1200000	15.56	-4.14E-03	15.56	-0.064
1400000	15.63	-4.84E-03	15.63	-0.076
1600000	15.69	-5.65E-03	15.69	-0.089
1800000	15.80	-6.29E-03	15.80	-0.099
2000000	15.94	-7.04E-03	15.94	-0.112

**Figure F2** Nyquist plot of SPPO, DS = 31 membrane.

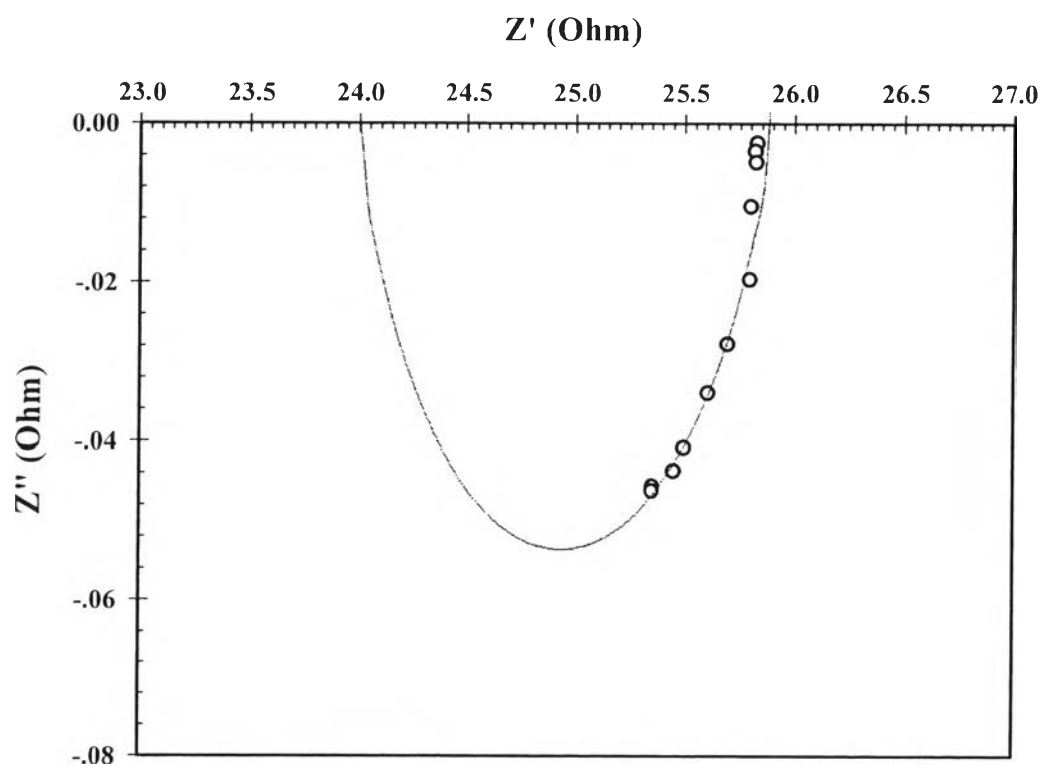
**Table F4** Proton conductivity raw data of calculations SPPO, DS = 31 membrane

Frequency, Hz	Z, ohm	r, Radian	Z'=Zcosr	Z''=Zsinr
80000	14.29	-4.95E-03	14.29	-0.071
100000	14.33	-5.62E-03	14.33	-0.081
200000	14.40	-8.43E-03	14.40	-0.121
400000	14.47	-1.30E-02	14.47	-0.188
600000	14.50	-1.70E-02	14.50	-0.247
800000	14.55	-2.04E-02	14.55	-0.297
1000000	14.61	-2.30E-02	14.60	-0.335
1200000	14.69	-2.60E-02	14.68	-0.382
1400000	14.76	-2.79E-02	14.76	-0.412
1600000	14.84	-2.97E-02	14.83	-0.441
1800000	14.89	-3.07E-02	14.88	-0.458
2000000	14.95	-3.18E-02	14.94	-0.475

**Figure F3** Nyquist plot of SPPO, DS = 31 membrane.

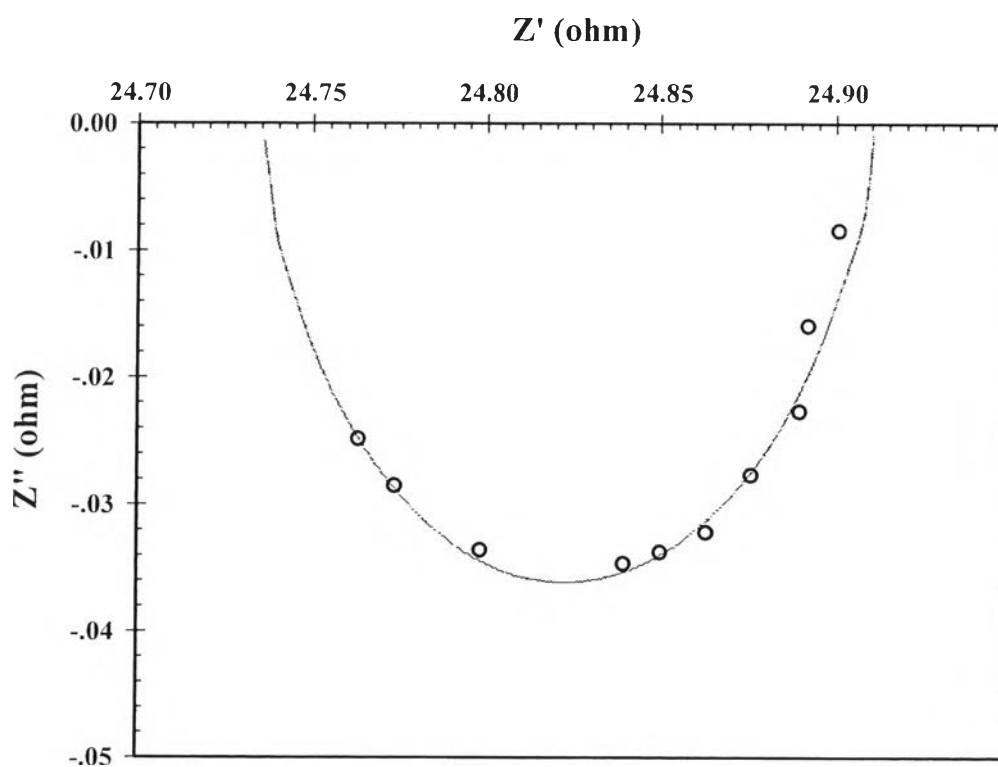
**Table F5** Proton conductivity raw data of calculations CM 0.1 %

Frequency, Hz	Z, ohm	r, Radian	Z'=Zcosr	Z''=Zsinr
60000	25.83	-9.97E-05	25.83	-0.003
80000	25.82	-1.40E-04	25.82	-0.004
100000	25.83	-1.93E-04	25.83	-0.005
200000	25.80	-4.09E-04	25.80	-0.011
400000	25.80	-7.66E-04	25.80	-0.020
600000	25.70	-1.09E-03	25.70	-0.028
800000	25.61	-1.33E-03	25.61	-0.034
1000000	25.50	-1.61E-03	25.50	-0.041
1200000	25.46	-1.72E-03	25.46	-0.044
1400000	25.36	-1.81E-03	25.36	-0.046
1600000	25.36	-1.83E-03	25.36	-0.046

**Figure F4** Nyquist plot of CM 0.1 %.

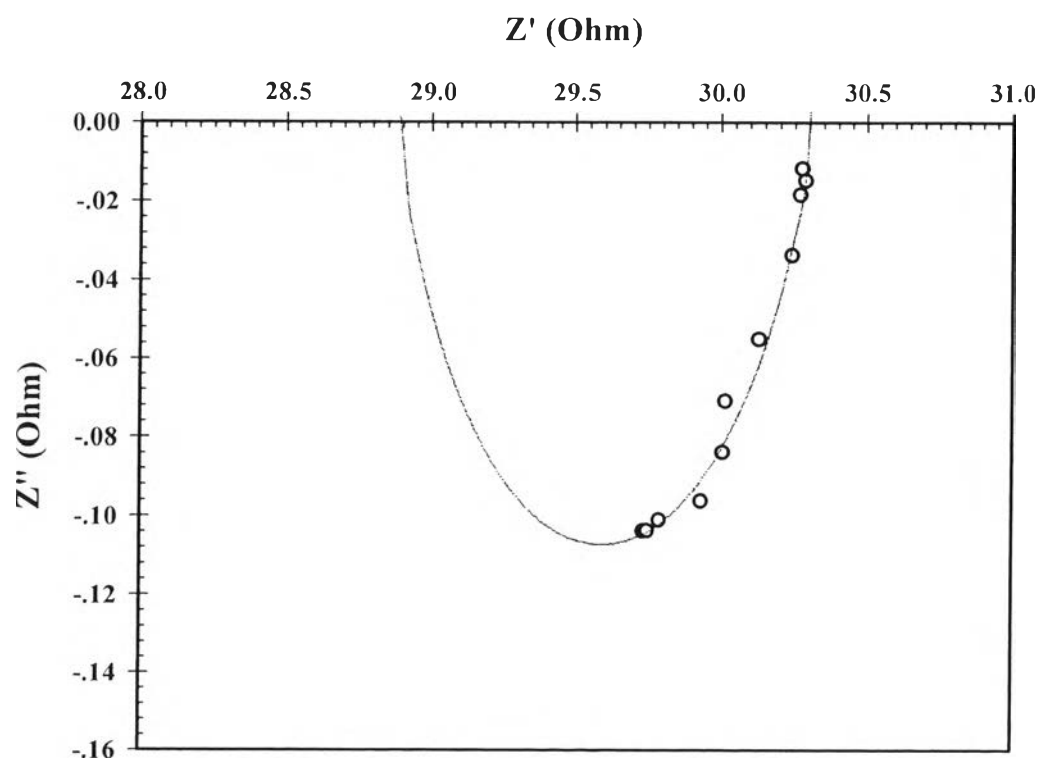
**Table F6** Proton conductivity raw data of calculations CM 0.1 %

Frequency, Hz	Z, ohm	r, Radian	Z'=Zcosr	Z''=Zsinr
200000	24.90	-3.42E-04	24.90	-0.009
400000	24.89	-6.44E-04	24.90	-0.016
600000	24.89	-9.15E-04	24.89	-0.023
800000	24.88	-1.12E-03	24.88	-0.0278
1000000	24.86	-1.30E-03	24.86	-0.032
1200000	24.85	-1.36E-03	24.85	-0.034
1400000	24.84	-1.40E-03	24.84	-0.035
1600000	24.80	-1.36E-03	24.80	-0.034
1800000	24.77	-1.16E-03	24.77	-0.029
2000000	24.76	-1.01E-03	24.76	-0.025

**Figure F5** Nyquist plot of CM 0.1 %.

**Table F7** Proton conductivity raw data of calculations CM 0.5 %

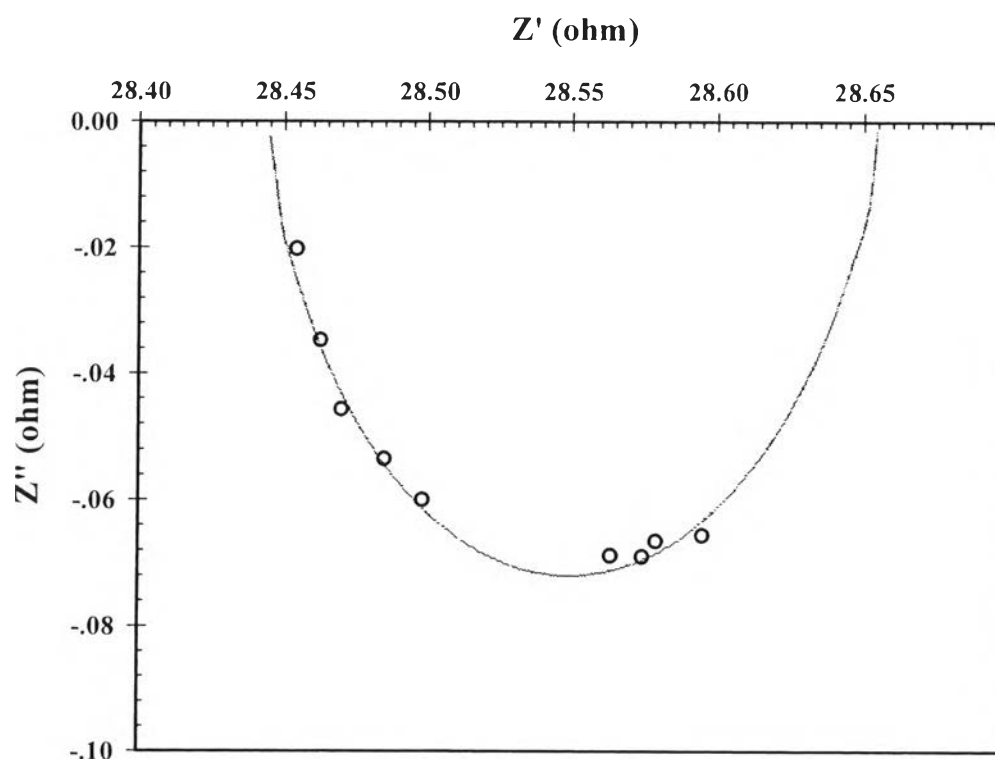
Frequency, Hz	Z, ohm	r, Radian	Z'=Zcosr	Z''=Zsinr
60000	30.28	-3.94E-04	30.28	-0.012
80000	30.29	-4.94E-04	30.29	-0.015
100000	30.27	-6.12E-04	30.27	-0.019
200000	30.24	-1.12E-03	30.24	-0.034
400000	30.13	-1.83E-03	30.13	-0.055
600000	30.02	-2.37E-03	30.02	-0.071
800000	30.01	-2.80E-03	30.01	-0.084
1000000	29.94	-3.22E-03	29.94	-0.096
1200000	29.79	-3.40E-03	29.79	-0.101
1400000	29.74	-3.50E-03	29.74	-0.104
1600000	29.75	-3.49E-03	29.75	-0.104

**Figure F6** Nyquist plot of CM 0.5 %.



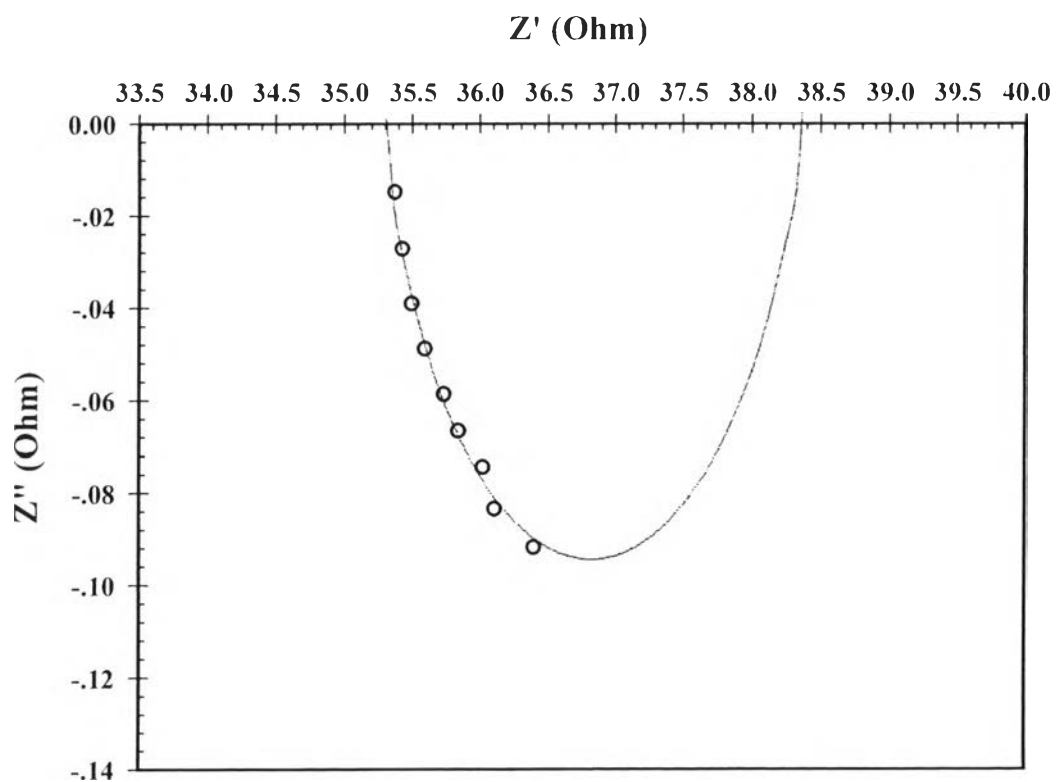
**Table F8** Proton conductivity raw data of calculations CM 0.5 %

Frequency, Hz	Z, ohm	r, Radian	Z'=Zcosr	Z''=Zsinr
200000	28.45	-7.17E-04	28.45	-0.020
400000	28.46	-1.23E-03	28.46	-0.035
600000	28.47	-1.61E-03	28.47	-0.046
800000	28.49	-1.88E-03	28.49	-0.054
1000000	28.50	-2.11E-03	28.50	-0.060
1200000	28.58	-2.33E-03	28.58	-0.067
1400000	28.56	-2.41E-03	28.56	-0.069
1600000	28.58	-2.42E-03	28.58	-0.069
1800000	28.60	-2.30E-03	28.60	-0.066

**Figure F7** Nyquist plot of CM 0.5 %.

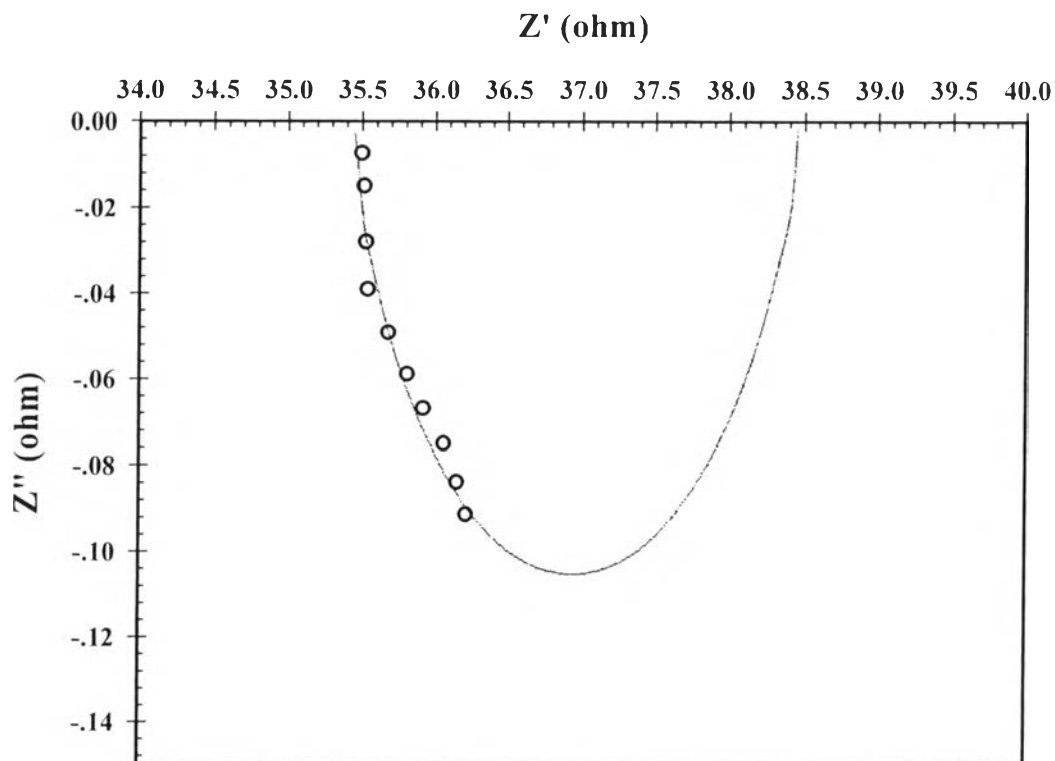
**Table F9** Proton conductivity raw data of calculations CM 1 %

Frequency, Hz	Z, ohm	r, Radian	Z'=Zcosr	Z''=Zsinr
200000	35.38	-4.26E-04	35.38	-0.015
400000	35.44	-7.73E-04	35.44	-0.027
600000	35.51	-1.11E-03	35.51	-0.039
800000	35.60	-1.38E-03	35.60	-0.049
1000000	35.75	-1.65E-03	35.75	-0.059
1200000	35.85	-1.86E-03	35.85	-0.067
1400000	36.03	-2.07E-03	36.03	-0.075
1600000	36.12	-2.31E-03	36.12	-0.084
1800000	36.41	-2.53E-03	36.41	-0.092

**Figure F8** Nyquist plot of CM 1 %.

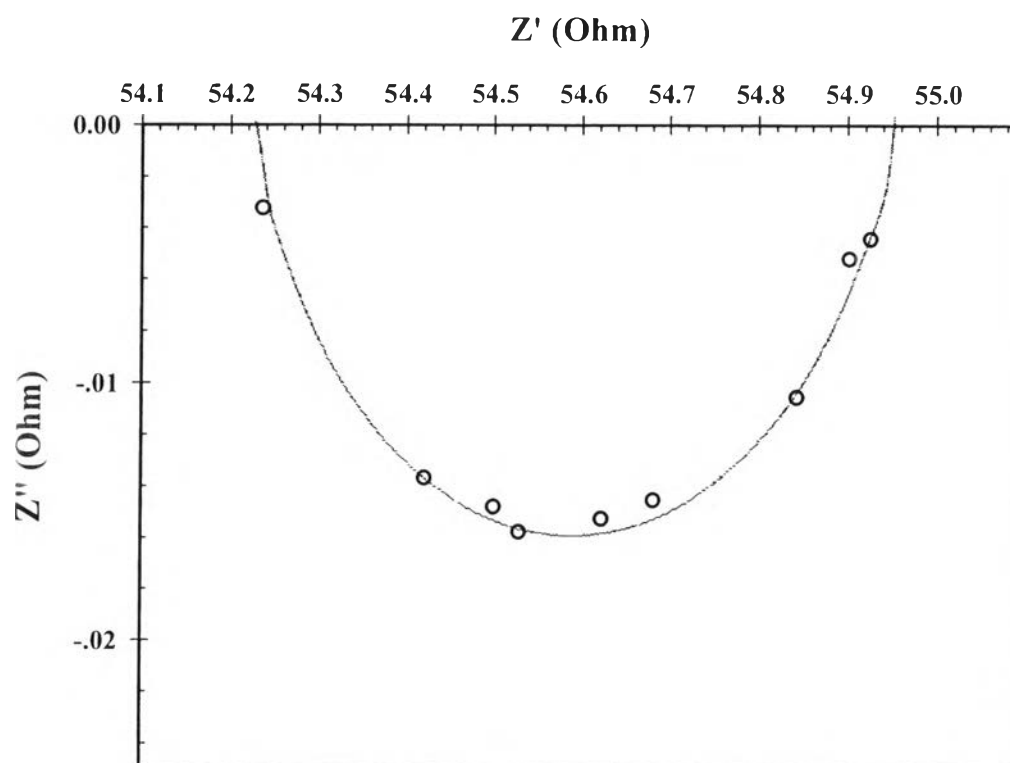
**Table F10** Proton conductivity raw data of calculations CM 1 %

Frequency, Hz	Z, ohm	r, Radian	Z'=Zcosr	Z''=Zsinr
100000	35.50	-2.14E-04	35.50	-0.008
200000	35.52	-4.27E-04	35.52	-0.015
400000	35.53	-7.93E-04	35.53	-0.028
600000	35.55	-1.10E-03	35.55	-0.039
800000	35.69	-1.38E-03	35.69	-0.049
1000000	35.82	-1.65E-03	35.82	-0.059
1200000	35.93	-1.87E-03	35.93	-0.067
1400000	36.07	-2.09E-03	36.07	-0.075
1600000	36.16	-2.32E-03	36.16	-0.084
1800000	36.22	-2.53E-03	36.22	-0.092

**Figure F9** Nyquist plot of CM 1 %.

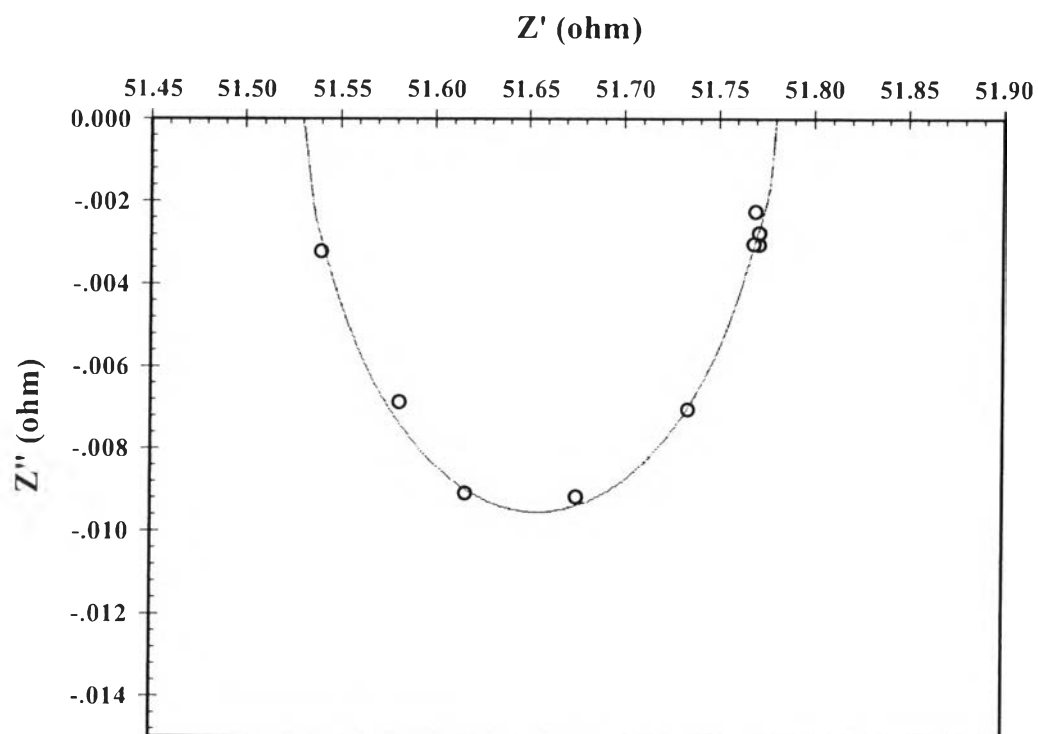
**Table F11** Proton conductivity raw data of calculations CM 2 %

Frequency, Hz	Z, ohm	r, Radian	Z'=Zcosr	Z''=Zsinr
6000	54.93	-8.13E-05	54.93	-0.004
8000	54.90	-9.55E-05	54.90	-0.005
10000	54.84	-1.93E-04	54.84	-0.011
20000	54.68	-2.66E-04	54.68	-0.015
40000	54.62	-2.80E-04	54.62	-0.015
60000	54.53	-2.90E-04	54.53	-0.016
80000	54.50	-2.72E-04	54.50	-0.015
100000	54.42	-2.52E-04	54.42	-0.014
200000	54.24	-6.05E-05	54.24	-0.003

**Figure F10** Nyquist plot of CM 2 %.

**Table F12** Proton conductivity raw data of calculations CM 2 %

Frequency, Hz	Z, ohm	r, Radian	Z'=Zcosr	Z''=Zsinr
4000	51.77	-5.40E-05	51.77	-0.003
6000	51.77	-5.95E-05	51.77	-0.003
8000	51.77	-4.41E-05	51.77	-0.002
10000	51.77	-5.92E-05	51.77	-0.003
20000	51.73	-1.37E-04	51.73	-0.007
40000	51.68	-1.78E-04	51.68	-0.009
60000	51.62	-1.77E-04	51.62	-0.009
80000	51.58	-1.34E-04	51.58	-0.007
100000	51.54	-6.30E-05	51.54	-0.003

**Figure F11** Nyquist plot of CM 2 %.

## Appendix G Methanol permeability

The methanol permeability of SPPO membrane was determined by a liquid permeation cell where the concentration of methanol that permeated the cell at 60 °C was measured. The liquid permeation cell is composed of two components. The two components were separated by a membrane sample. Compartment A was filled with methanol at 2.5 M 250 ml and a compartment B was filled with DI water 250 ml. The two solutions were continuously stirred during the measurement. The methanol concentration was determined by using the gas chromatography. The methanol permeability coefficient was calculated from the following equation:

$$P = \frac{k_B V_B L}{A(C_A - C_B)} \quad (G1)$$

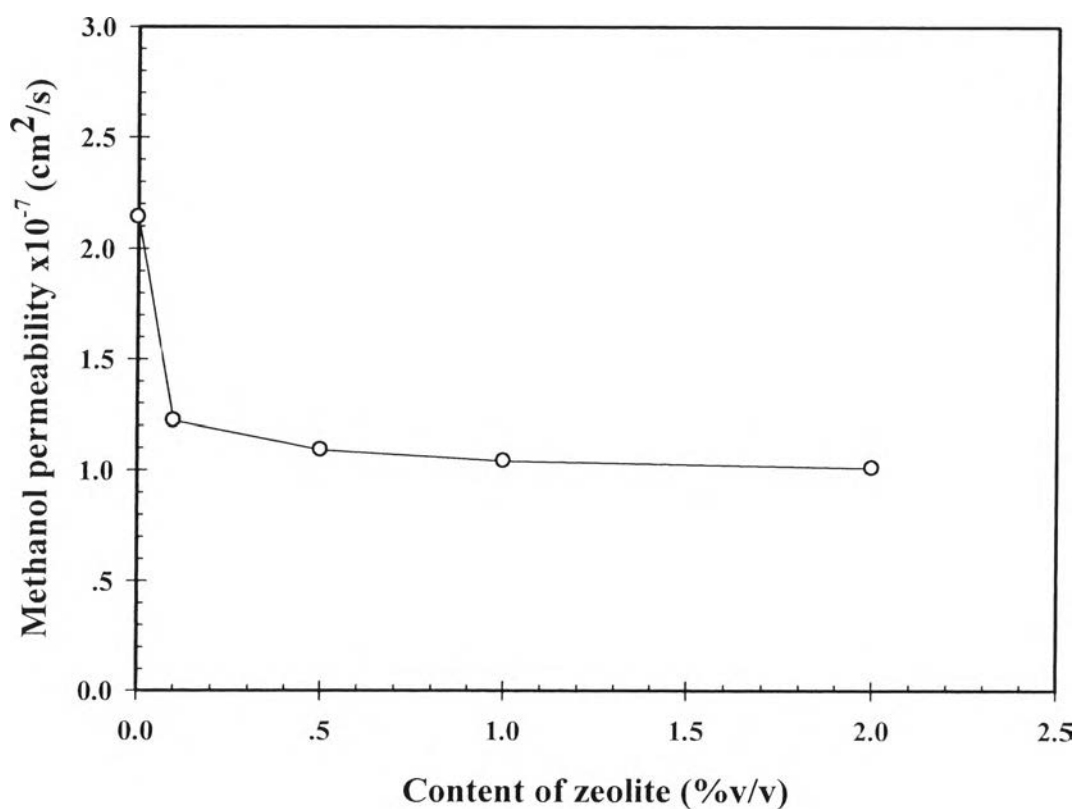
where

- $P$  = the methanol permeability ( $\text{cm}^2/\text{s}$ )
- $C_A$  = the methanol concentrations in the compartment A
- $C_B$  = the methanol concentrations in the compartment B
- $k_B$  = the methanol concentration permeate per time of permeate (the slope of methanol concentration profile in the compartment B)
- $V_B$  = the solution volume of the permeate
- $L$  = the thickness of the membrane
- $A$  = the effective area of membrane

The methanol concentration profile was obtained by using a PR2100 gas chromatography fitted with a Thermal Conductivity Detector (TCD). The internal standard was 0.1 M of ethanol (Zhai *et al.*, 2007).

**Table G1** Methanol permeability of SPPO and composite membranes at various concentrations

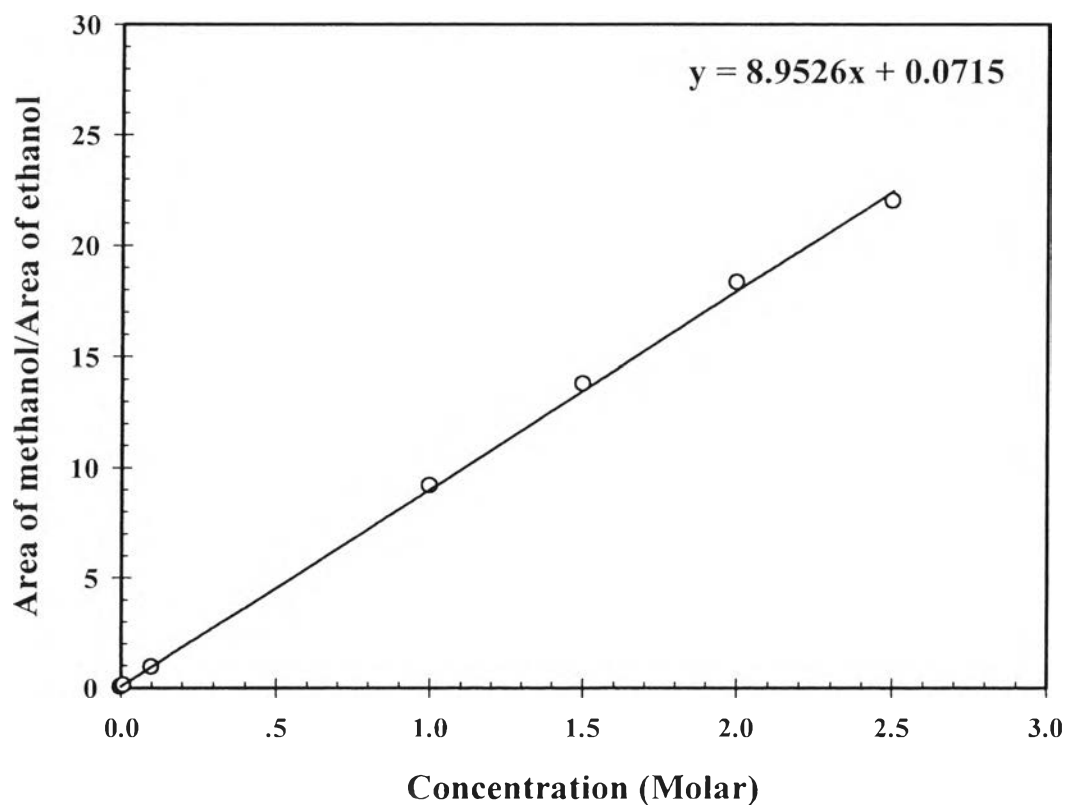
Composite membranes (%v/v)	Thickness, $L$ (cm)	Slope, $k_B$ (mol/L.s)	Methanol permeability, $P$ (cm <sup>2</sup> /s)
SPPO, DS = 31	$1.51 \times 10^{-2}$	$6.61 \times 10^{-7}$	$2.14 \times 10^{-7}$
CM 0.1 %	$1.50 \times 10^{-2}$	$3.78 \times 10^{-7}$	$1.22 \times 10^{-7}$
CM 0.5 %	$1.55 \times 10^{-2}$	$3.26 \times 10^{-7}$	$1.09 \times 10^{-7}$
CM 1 %	$1.72 \times 10^{-2}$	$2.82 \times 10^{-7}$	$1.04 \times 10^{-7}$
CM 2 %	$1.80 \times 10^{-2}$	$2.61 \times 10^{-7}$	$1.01 \times 10^{-7}$
Nafion 117 (Woo <i>et al.</i> , 2003)	$1.75 \times 10^{-2}$	-	$2.38 \times 10^{-6}$



**Figure G1** The methanol permeability of composite membranes as a function of content of zeolite.

**Table G2** Raw data of internal standard curve of methanol concentration

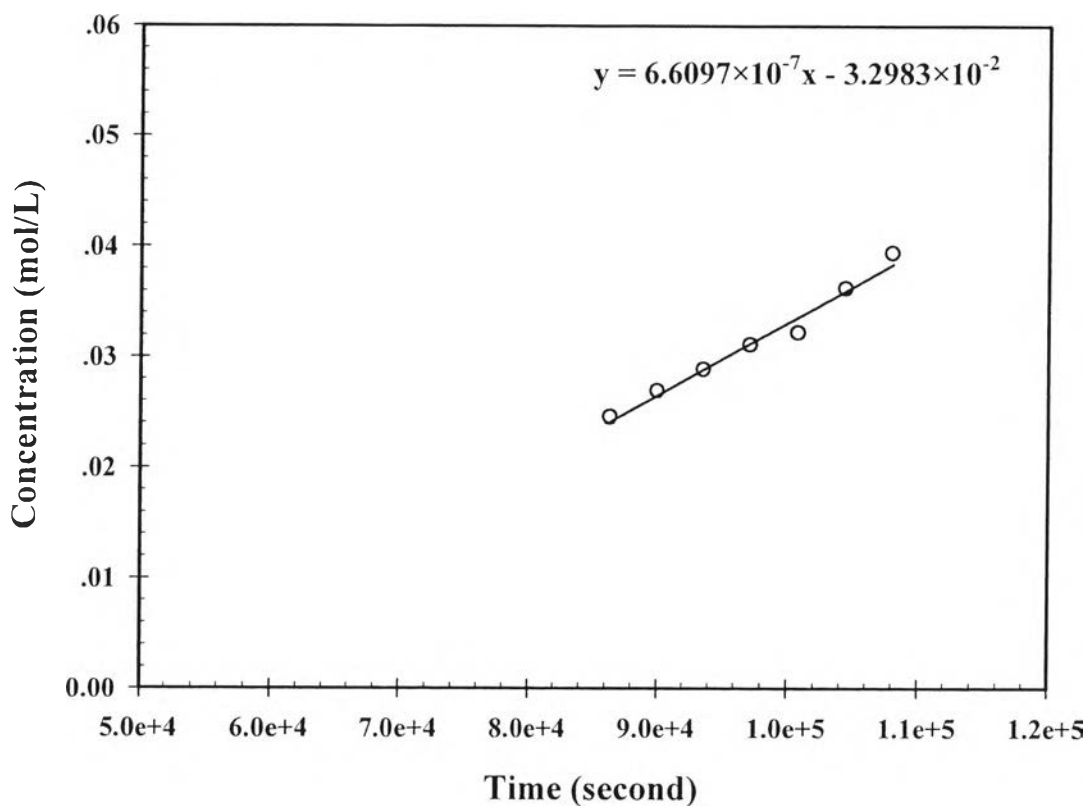
Methanol concentration	Peak area of methanol		Peak area of ethanol		Peak area ratio	
	No.1	No.2	No.1	No.2	No.1	No.2
0.0001 M	0.01	0.01	1.74	1.14	0.006	0.009
0.001 M	0.03	0.03	1.77	1.98	0.017	0.015
0.01 M	0.15	0.13	1.62	1.66	0.093	0.078
0.1 M	1.64	1.68	1.78	1.87	0.921	0.898
1 M	17.37	15.45	1.75	1.83	9.926	8.443
1.5 M	26.78	21.29	1.75	1.74	15.30	12.24
2 M	32.64	28.67	1.61	1.74	20.27	16.48
2.5 M	41.14	36.87	1.67	1.88	24.63	19.61

**Figure G2** Internal standard curve of methanol concentration.



**Table G3** Raw data of methanol permeability calculation of SPPO, DS = 31 membrane

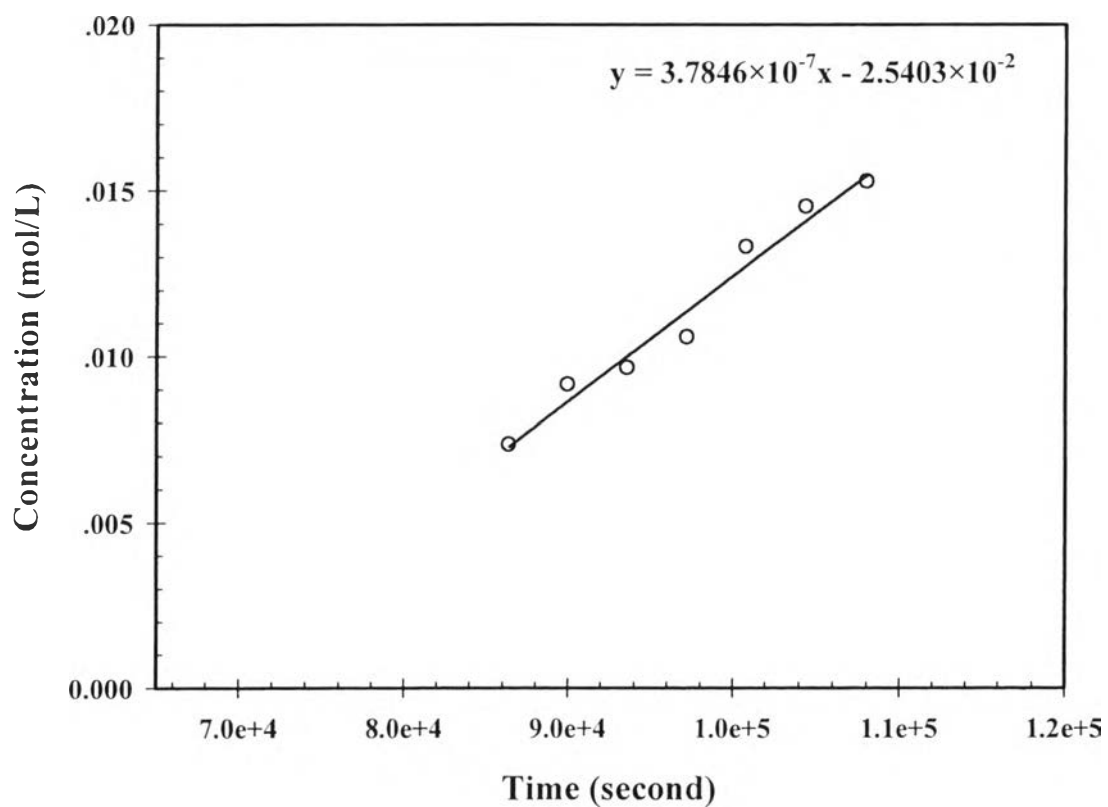
Time (second)	Methanol concentration (M)	
	Comp. A	Comp. B
86400	2.488	0.012
90000	2.476	0.024
93600	2.473	0.027
97200	2.471	0.029
100800	2.469	0.031
104400	2.468	0.032
108000	2.464	0.036



**Figure G3** Methanol concentration in compartment B vs. time (s) of SPPO, DS = 31 membrane.

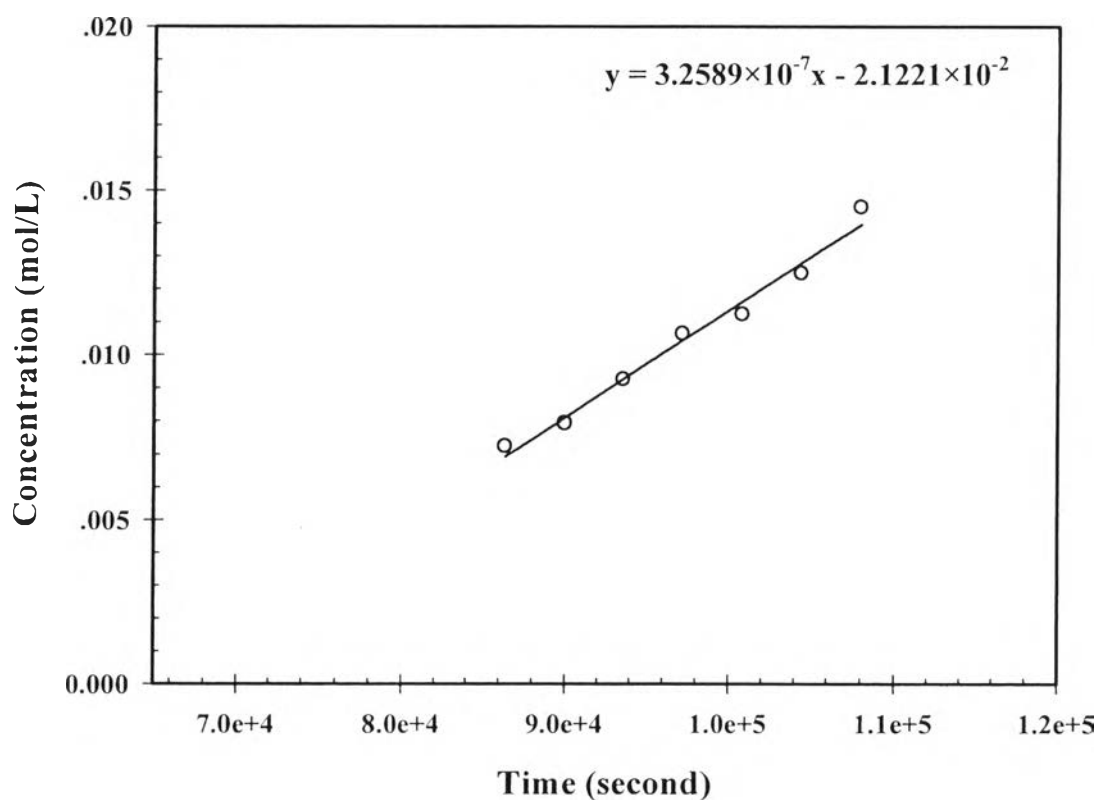
**Table G4** Raw data of methanol permeability calculation of CM 0.1 %

Time (second)	Methanol concentration (M)	
	Comp. A	Comp. B
86400	2.493	0.007
90000	2.491	0.009
93600	2.490	0.010
97200	2.489	0.011
100800	2.487	0.013
104400	2.486	0.014
108000	2.485	0.015

**Figure G4** Methanol concentration in compartment B vs. time (s) of CM 0.1 %.

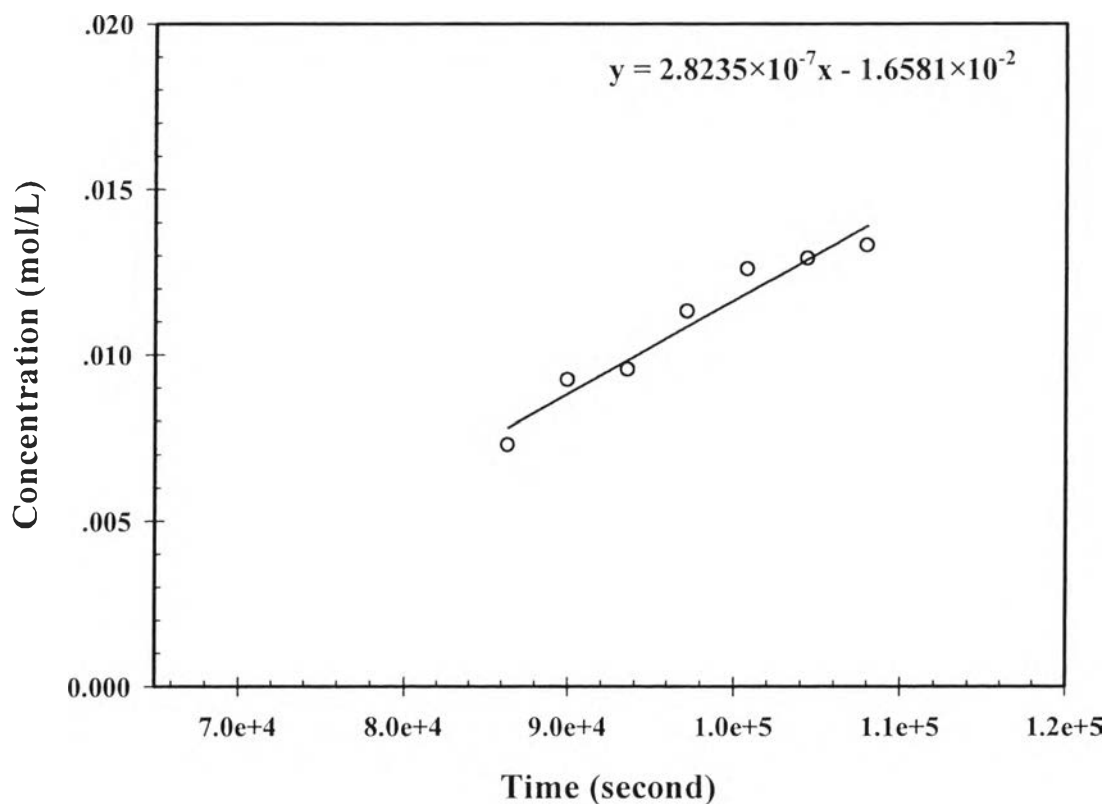
**Table G5** Raw data of methanol permeability calculation of CM 0.5 %

Time (second)	Methanol concentration (M)	
	Comp. A	Comp. B
86400	2.493	0.007
90000	2.492	0.008
93600	2.491	0.009
97200	2.490	0.011
100800	2.489	0.011
104400	2.488	0.012
108000	2.486	0.014

**Figure G5** Methanol concentration in compartment B vs. time (s) of CM 0.5 %.

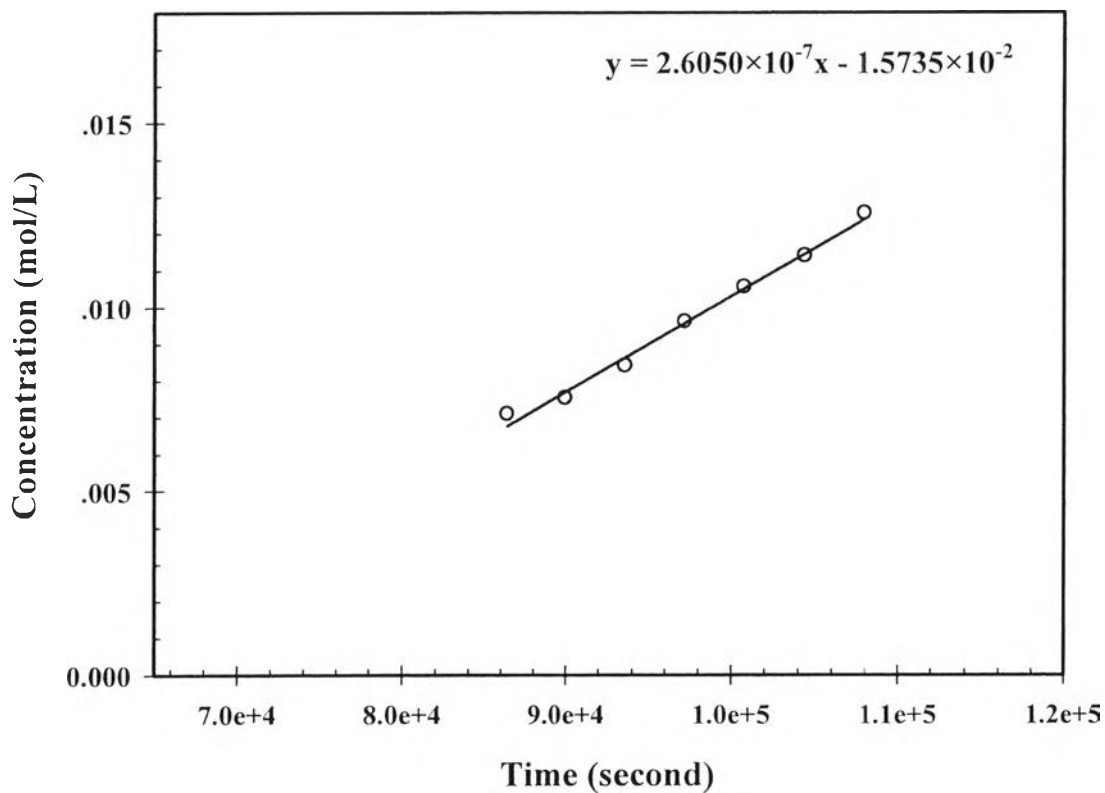
**Table G6** Raw data of methanol permeability calculation of CM 1 %

Time (second)	Methanol concentration (M)	
	Comp. A	Comp. B
86400	2.493	0.007
90000	2.491	0.009
93600	2.490	0.010
97200	2.489	0.011
100800	2.487	0.013
104400	2.487	0.013
108000	2.487	0.013

**Figure G6** Methanol concentration in compartment B vs. time (s) of CM 1 %.

**Table G7** Raw data of methanol permeability calculation of CM 2 %

Time (second)	Methanol concentration (M)	
	Comp. A	Comp. B
86400	2.493	0.007
90000	2.492	0.008
93600	2.492	0.008
97200	2.490	0.010
100800	2.489	0.011
104400	2.489	0.011
108000	2.487	0.013

**Figure G7** Methanol concentration in compartment B vs. time (s) of CM 2 %.

## Appendix H Membrane selectivity

The membrane selectivity, which is defined as the ratio of proton conductivity to methanol permeability, is used to determine the potential performance of DMFC membranes. Membrane which has higher selectivity parameter is high performance for DMFC application. The membrane selectivity values of SPPO and the composite membranes were compared with those of Nafion 117 (Sadrabadi *et al.*, 2009).

**Table H1** Membrane selectivity of SPPO and composite membranes at various concentrations

Composite membranes (%v/v)	Proton Conductivity, $\sigma$ (S/cm)	Methanol permeability, P (cm <sup>2</sup> /s)	Membrane selectivity (S.s/cm <sup>3</sup> )
SPPO, DS = 31	$1.00 \times 10^{-2}$	$2.14 \times 10^{-7}$	46729
CM 0.1 %	$7.34 \times 10^{-3}$	$1.22 \times 10^{-7}$	60164
CM 0.5 %	$5.80 \times 10^{-3}$	$1.09 \times 10^{-7}$	53211
CM 1 %	$5.59 \times 10^{-3}$	$1.04 \times 10^{-7}$	53750
CM 2 %	$4.54 \times 10^{-3}$	$1.01 \times 10^{-7}$	44950
Nafion 117 (Woo <i>et al.</i> , 2003)	$1.00 \times 10^{-1}$	$2.38 \times 10^{-6}$	42017

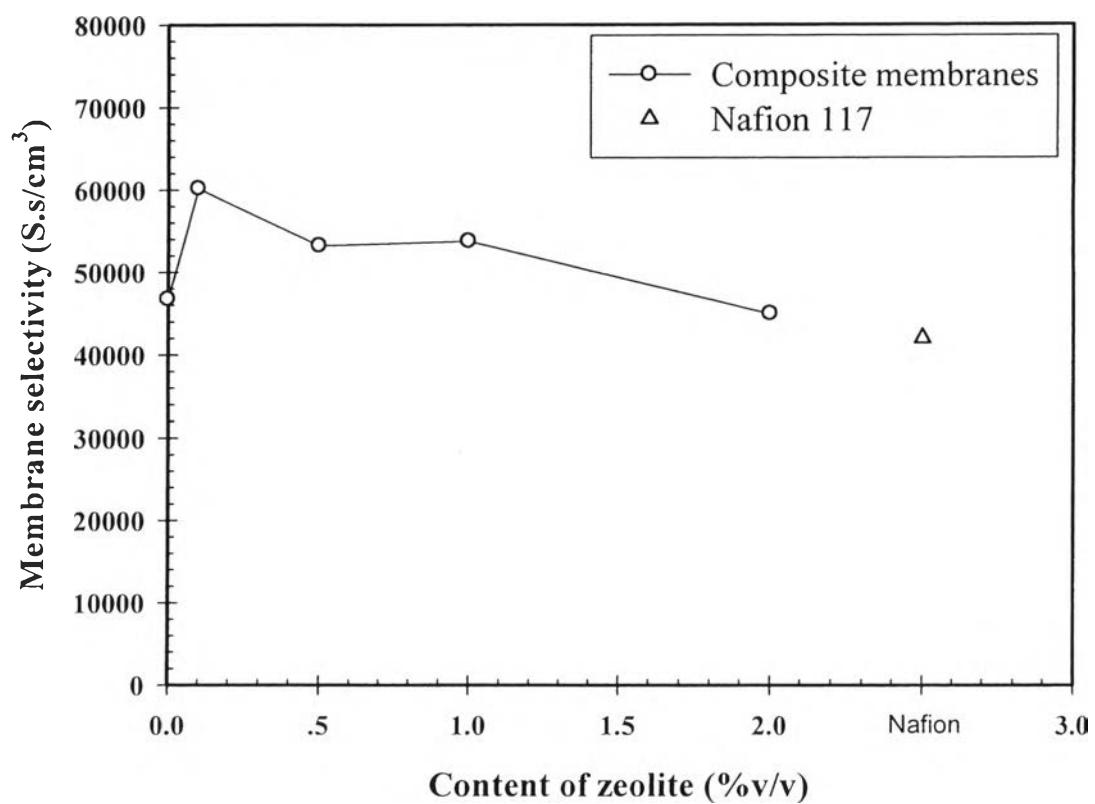


**Figure H1** Membrane selectivity of composite membranes at various concentrations and Nafion 117.

## Appendix I Mechanical property

The tensile strength of SPPO and the composite membranes was determined by using a Universal Testing Machine (Lloyd, model SMT2-500N) for characterization of the mechanical property. The samples were cut into size 1cm × 5cm and using the gauge length of 3 cm. The membranes were immersed in de-ionized water for 24 h before testing and using the speed of 10 mm/min (Macksasitorn *et al.*, 2012).

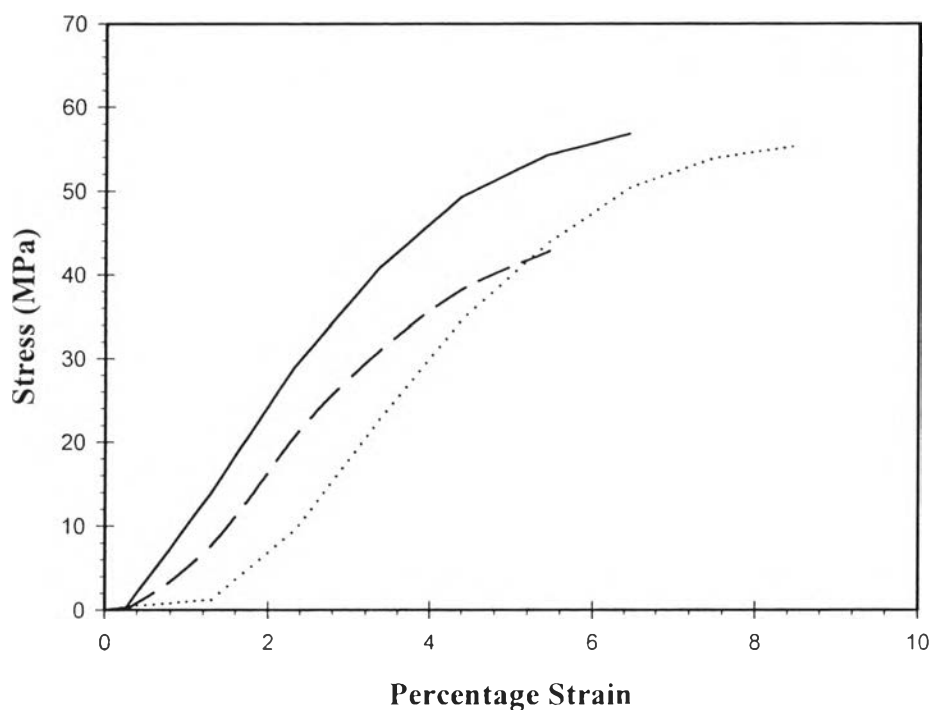
**Table II** Mechanical properties of composite membranes

<b>Composite membranes (%v/v)</b>	<b>Tensile strength (MPa)</b>	<b>Young's modulus (GPa)</b>	<b>Elongation at break (%)</b>	<b>Stiffness (N/m)</b>
SPPO, DS = 31	51.78	1.51	6.81	34228.38
CM 0.1 %	42.64	1.25	6.10	56532.61
CM 0.5 %	36.69	1.36	5.11	64034.34
CM 1 %	28.65	1.66	3.00	89435.38
CM 2 %	12.58	1.79	1.31	116706.51
Nafion 117 (Liu <i>et al.</i> , 2007)	28.40	1.00	329.20	-



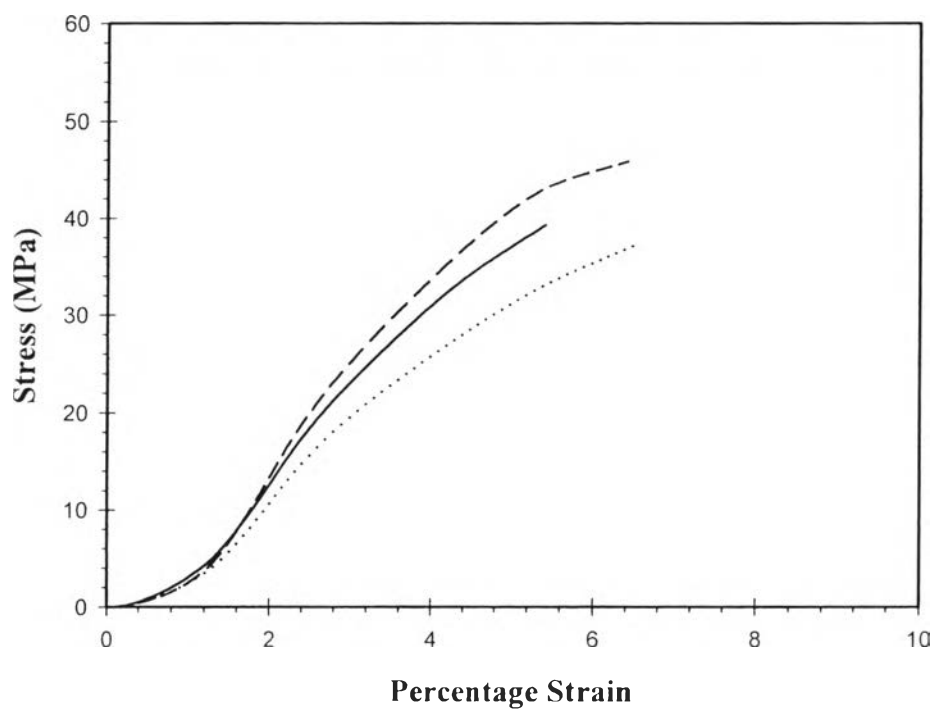
**Table I2** Mechanical properties of SPPO, DS = 31 membranes

Polymer	Tensile strength (MPa)	Young's modulus (MPa)	Elongation at break (%)	Stiffness (N/m)
SPPO, DS = 31	55.49	1321.17	6.45	31708.03
	42.86	1401.99	8.52	32713.09
	57.01	1793.63	5.46	38264.01
Average	51.79±7.77	1505.59±206.32	6.81±1.57	34228.38±3530.90

**Figure I1** Stress-strain behavior of SPPO, DS = 31 membrane.

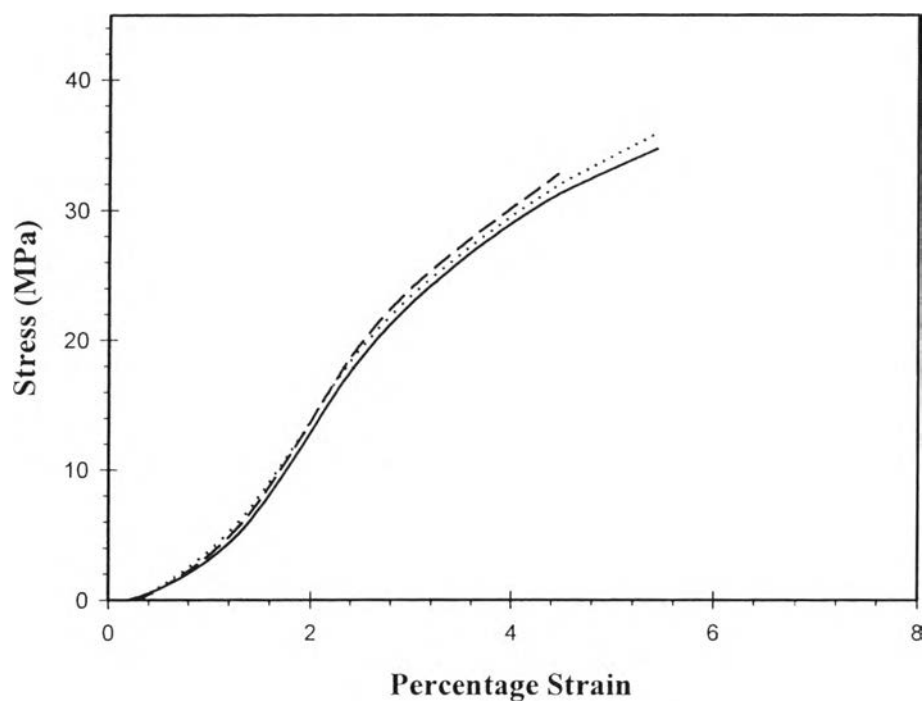
**Table I3** Mechanical properties of CM 0.1 %

Polymer	Tensile strength (MPa)	Young's modulus (MPa)	Elongation at break (%)	Stiffness (N/m)
CM 0.1 %	43.33	1198.26	5.41	54321.23
	38.05	1105.72	6.48	54917.61
	46.56	1448.62	6.42	60358.98
Average	42.64±4.29	1250.87±177.40	6.10±0.60	56532.61±3327.12

**Figure I2** Stress-strain behavior of CM 0.1 % membrane.

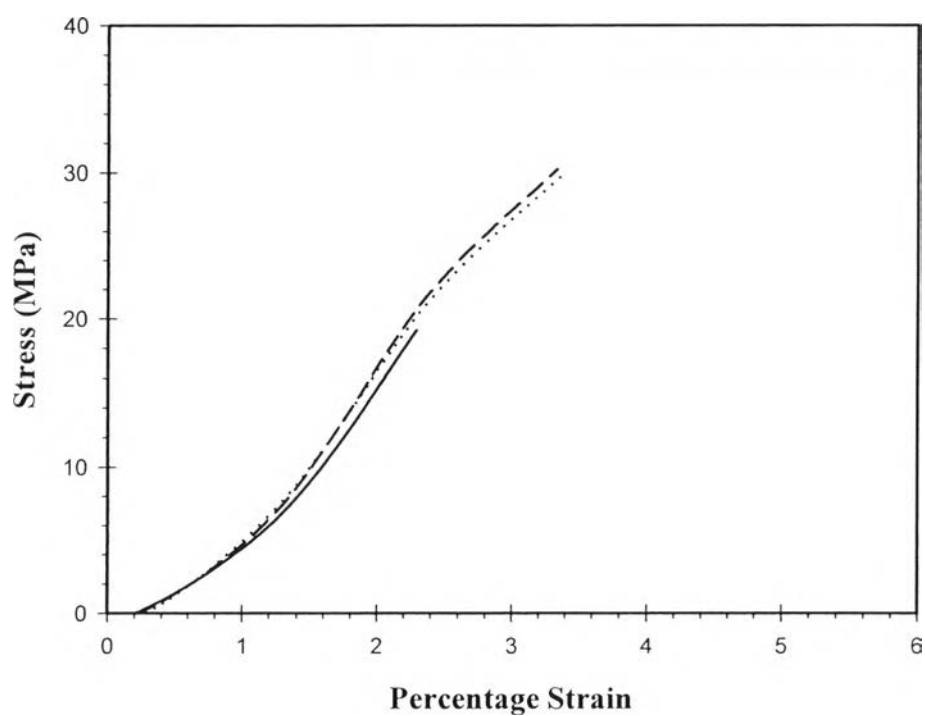
**Table I4** Mechanical properties of CM 0.5 %

Polymer	Tensile strength (MPa)	Young's modulus (MPa)	Elongation at break (%)	Stiffness (N/m)
CM 0.5 %	36.91	1281.67	5.42	60665.74
	36.99	1374.39	5.44	67803.25
	36.17	1435.35	4.46	63634.05
Average	36.69±0.45	1363.81±77.39	5.11±0.57	64034.34±3585.55

**Figure I3** Stress-strain behavior of CM 0.5 % membrane.

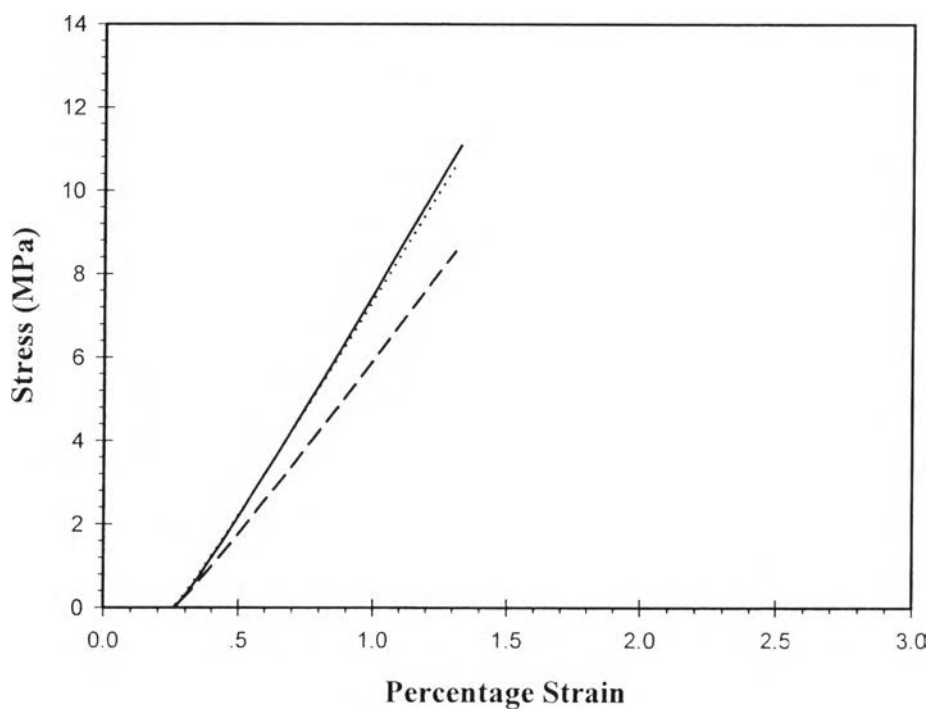
**Table I5** Mechanical properties of CM 1 %

Polymer	Tensile strength (MPa)	Young's modulus (MPa)	Elongation at break (%)	Stiffness (N/m)
CM 1 %	22.68	1582.74	2.29	79136.90
	30.55	1656.76	3.38	93883.05
	32.72	1753.73	3.34	95286.18
Average	28.65±5.28	1664.41±85.75	3.00±0.62	89435.38±8946.29

**Figure I4** Stress-strain behavior of CM 1 % membrane.

**Table I6** Mechanical properties of CM 2 %

Polymer	Tensile strength (MPa)	Young's modulus (MPa)	Elongation at break (%)	Stiffness (N/m)
CM 2 %	16.27	1374.41	1.33	98957.45
	12.47	1519.18	1.30	107861.64
	8.99	2484.98	1.31	143300.42
Average	12.58±3.64	1792.86±603.75	1.31±0.01	116706.51±23457.37

**Figure I5** Stress-strain behavior of CM 2 % membrane.

## CURRICULUM VITAE

**Name:** Mr. Piyanat Kotaphan

**Date of Birth:** October 21, 1988

**Nationality:** Thai

**University Education:**

2007-2010 Bachelor Degree of Science (Applied Chemistry), Faculty of Science, Rangsit University, Pathumthani, Thailand

**Proceedings:**

1. Kotaphan, P., Sirivat, A. and J. Schwank. (2013, April) Composite Membrane of Sulfonated Poly(2,6-dimethyl-1,4-phenylene oxide) and Zeolite for Direct Methanol Fuel Cell Applications. Proceeding of the 4<sup>th</sup> Research Symposium on Petrochemical and Materials Technology and The 19<sup>th</sup> PPC Symposium on Petroleum, Petrochemicals, and Polymers, Ballroom, Queen Sirikit National Convention Center, Bangkok, Thailand.

**Presentation:**

1. Kotaphan, P., Sirivat, A. and J. Schwank. (2013, April) Composite Membrane of Sulfonated Poly(2,6-dimethyl-1,4-phenylene oxide) and Zeolite for Direct Methanol Fuel Cell Applications. Paper Presented at The 1<sup>st</sup> Annual Symposium Conductive and Electroactive Polymer, Bangkok, Thailand.
2. Kotaphan, P., Sirivat, A. and J. Schwank. (2013, April) Composite Membrane of Sulfonated Poly(2,6-dimethyl-1,4-phenylene oxide) and Zeolite for Direct Methanol Fuel Cell Applications. Paper Presented at The 4<sup>th</sup> Research Symposium on Petrochemical and Materials Technology and the 19<sup>th</sup> PPC Symposium on Petroleum, Petrochemicals, and Polymers, Bangkok, Thailand.
3. Kotaphan, P., Sirivat, A. and J. Schwank. (2013, May) Sulfonated Poly(2,6-dimethyl-1,4-phenylene oxide) Composite Membranes filled by Zeolite for Direct Methanol Fuel Cell. Paper Presented at The 3<sup>rd</sup> International Symposium Frontiers in Polymer Science In association with the journal polymer, Sitges, Spain.